BEAMLINE AND ACCELERATOR DEVELOPMENT

CYCLOTRON OPERATING SUMMARY - 1ST PERIOD

E. Kashy, P. Miller, D. Poe, G. Humenik,
L. Wilkinson and N. Friedman

The first beam was extracted from the K-500 cyclotron on August 31, 1982. This was a 106 MeV deuteron beam, and was followed by some operation with 225 MeV 4 He +2 beams. A beam of 35 MeV/A ^{12}C was then accelerated and an elastic scattering measurement from a gold target using a Si counter telescope in the 60" scattering chamber showed a beam spread of ~0.1%. Operating experience during the first ten weeks revealed a number of problem areas which needed attention before the experimental program could seriously begin.

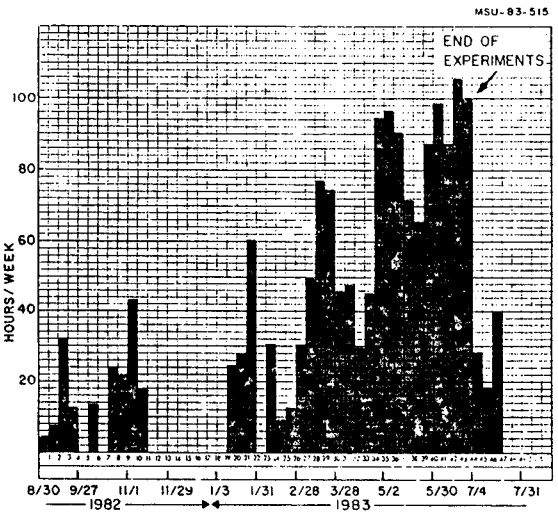

Fig. 1.

Figure 1 shows the record of extracted beams out of the cyclotron from the initial extraction to the end of the first operating perioed - with over 900 hours of that time used successfully for experiments. A look at Figure 1 shows the rather difficult operation for the first ten weeks. The principal problem identified was that of cryopumping. It is discussed in detail elsewhere. The gap that follows represents the shutdown, where a number of changes in the cyclotron were made. In the weeks that followed we encountered some problems with our cryogenics refrigerator which were resolved. In the last 10 weeks, operation was excellent, with tome on target at about 90% of scheduled time.

During this period, a total of 18 different beams of six isotopes were developed and run. The experimental program successfully used four of the six beam stations, with the Enge split pole and RPMS yet to be used for experiments. Table 1 is a summary of time used during the first running period in the experimental program.

The operation of the K-500 during this first period uncovered or confirmed a number of problem areas. It also provided time to consider and prepare to implement the needed modifications. The problems included cryopumping, cryodistribution, ion source activation, and high voltage operation of electrostatic deflectors. In the case of the ion source for example, spare ion sources are being constructed and shields are being incorporated in the new design. Details of the projects, most of which are planned for the shut-down in August and September 1983 are found elsewhere in this report.

In considering operation for the next period we are keeping in mind the following goals/functions for the K-500. 1) To provide beams for approved experiments 2) to provide tests for systems to be used in the K-800 cyclotron and 3) to develop the injector mode beams which will be used in the coupled cyclotrons operation.

EXP	SPOKESPSN	TIME REQUESTED	TIME ALLOTTED	TTL	STATION	NOTE	PART AT WT	PART TYPE	ENERGY	TIME	DATE	RUN
82001	SEABORG	48	24	28	M-1	1	12	C	35	6	02/19	1
							12	C	35	10	02/22	2
							12	C	35	12	05/18	3
82003	PARKINSON	4	4	8	USERS	1	12	C	30	8	03/01	1
82004	NAMBOODIRI	32	32	0	SC	2						1
82008	WESTFALL	200	100	36	SC	1	12	C	30	10	11/04	1
							12	C	25	11	11/04	2
							4	He	25	5	01/25	3
							12	C	25	10	01/25	4
82009	ANANTARAMAN	120	60	40	SC	3	22	Ne	25	15	04/09	1
							22	Ne	15	6	04/20	2
							4	He	25	8	04/07	3
							12	C	25	11	04/08	4
82011	BRAUN-MUNZINGER	24	24	112	USERS	1	14	N	35	112	06/27	1
82012	SCHRODER	120	120	64	NC	1	14	N	35	64	06/22	1
82014	NOLEN	144	72	0	S-320	4				0		1
82015	HASSELQUIST	120	60	80	SC	1	12	C	30	76	04/25	1
							4	He	25	4	04/29	2
82018	GELBKE	144	24	60	SC	1	12	C	35	8	03/08	1
							12	C	30	32	03/11	2
82020	GELBKE	192	90	9P	SC	1	14	N	15	14	05/12	1
							14	N	25	9	05/13	2
							14	N	30	57	05/13	3
							14	N	20	12	05/13	4
							4	He	25	4	05/19	5
82030	HARWOOD	200	72	103	S-320	1	14	N	35	90	06/15	1
82032	GALONSKY	168	48	90	NC	1	14	N	35	90	06/15	1
82034	ANANTARAMAN	72	72	0	S-320	4	12	C	35	0	03/05	1
82038	SCHUBERT	16	16	28	M-1	1	14	N	25	4	02/08	1
							14	N	30	14	05/25	2
							14	N	15	8	06/08	3
							14	N	35	2	06/20	4
82040	WOLF	96	24	33	SC	1	14	N	25	10	06/06	1
							14	N	35	19	06/07	2
							14	N	15	4	06/08	3
82041	BECCHETTI	24	24	36	S-320	1	16	O	20	36	06/13	1
82050	McHARRIS			96	SC	5	14	N	15	14	05/09	1
							14	N	25	9	05/13	2
							14	N	30	57	05/13	3
							14	N	20	12	05/13	4
							4	He	25	4	05/19	5

1.) Ran successfully.

2.) Time offered on 03/07/83 but declined.

3.) Required pulsed ion source for 22 Ne +5. Experiment was run in conjunction with ion source development on and off for about four weeks. Seventeen ion sources used.

4.) Spent time debugging equipment (S320 Spectrograph).

5.) Parasitic time in scattering chamber beam. (Director's approval) Bombardment of Plutonium target. Shared with experiment # 82020.

STATUS OF CONTROL SYSTEM SOFTWARE DEVELOPMENT

R. Au, R. Fox, B. Jeltema, B. Johnson

Abstract

The current status of the control system for the k-500 cyclotron is discussed. An overview of the hardware and software configuration are also given.

1.0 INTRODUCTION

At an early stage in the K-500/K-800 planning, it was decided that these devices should be computer controlled. We felt that in view of the number of devices which are involved, and in view of the expense of cabling these devices to a central location, as would be required for a hard wired control system, computer control would in the long run be far more cost effective, and more flexible than a similar hard wired system.

The following response requirements strongly influenced the development of the project.

1. Approximately 1000 devices would be controlled by the final system. This included all devices on the K-500, K-800 cyclotrons as well as the associated beam lines and experimental facilities.
2. It should be possible to distribute the control areas so that physicists could control the portions of the experimental facilities which were involved in their experiments.
3. It should be possible to have multiple control devices attached to a controlled device (this is a direct consequence of the previous requirement).
4. Response to the operator should be in real time (~.1 seconds).
5. The system would look to the operator primarily like a hard wired control system with the exception of a very few 'smart' controllers or other smart functions. In particular, the use of knobs and meters for control and display devices was deemed superior to traditional computer input devices such as keypads and terminals.

The first section below gives the final computer hardware configuration as far as it influences the control system software development. The next section gives an overview of the software strategy used, while the last section gives summary of the development so far.

2.0 COMPUTER HARDWARE

The control system hardware finally chosen was based on a tightly coupled multiprocessor system. Each of the processors was chosen from the DEC PDP-11 family of minicomputers and had a specific set of duties to perform. Communications between the processors was by means of a shared multiport memory.

The processors chosen were two PDP-11/34's, and one PDP-11/45. The two 11/34's run as stand alone controllers for the console apparatus and the cyclotron apparatus, while the 11/45 performs general overseeing functions, and serves as the program development machine. The 11/34's run in a stand alone environment using the RSX-11S operating system. The RSX-11S system is a diskless variant of the RSX-11M system, which is run on the 11/45. Thus, the 11/45 possesses all of the mass storage devices (disks, tape drives), of the control system as well as the traditional input/output equipment (terminals, graphics displays and so on). All computers are equipped with 124Kw of memory with parity error detection. The processors communicate via 16Kw of 4-port memory. The control computers communicate with the outside world via a CAMAC serial highway which talks to the control computers via a Kinetics Systems Model 2050 serial highway driver. This device is a list processing DMA interface to a CAMAC serial highway (ANSII/IEEE Std 595-1982). To use it one sets up lists of valid CAMAC commands and points the 2050 at them. The output data is taken from the list, while the input data is placed in a data list.

The control system serial highway is topologically a two loop system. The console devices reside on one loop accessable to only the console 11/34, while the cyclotron devices reside on a second loop accessable only to the cyclo 11/34. The 11/45 can only directly talk to some K-500 main magnet monitoring devices.

3.0 CONTROL SYSTEM SOFTWARE

The basic software strategy has been to keep an up to date map of the control system status available at all times in the multiport memory. The console 11/34 is obligated to maintain the set of cells in the multiport memory corresponding to the values that are requested of the control devices, and is also responsible for monitoring the actual value cells in the multiport and displaying them on the console displays. The cyclotron 11/34 has similar obligations except that it must update the actual values in the multiport and use the requested values in the multiport to alter the condition of the control hardware. The control system software is divided logically in several segments.

1. Control software for the console (entirely in the console 11/34).
2. Control software for cyclotron devices (entirely in the cyclotron 11/34).

3. Control software for data acquisition and plotting (split between all computers)
4. Smart control/monitoring software (entirely in the 11/45).

3.1 Control Software For Console And Cyclotron Hardware

The control software for the console and cyclotron hardware is based on a simple polling system. Every .1 seconds, the console program reads all of the console devices and updates the requested values in the multiport memory. Similarly, it reads the current cyclotron values from the multiport memory and updates the console displays from them. The cyclotron program has much the same function, but instead reads the cyclotron devices using them to update cells in the multiport memory, while using the requested values set by the console program to update the requests it makes of the cyclotron hardware. All console devices are incremental, this allows multiple console devices to be attached to the same cyclotron device without conflict, since the effects of change are simply cumulative.

3.2 Control Software For Data Acquisition And Plotting

Currently there are two devices which require plots to be made of beam current against a sensor position. These are the K-500 main beam probe which runs on a track from the central region all the way through the extraction channel giving current as a function of radius, and a K-500 viewer probe which gives a detailed beam profile in and near the extraction radius. The control software for these plotting devices is common and is broken up into three pieces, a data acquisition and control program, a data spooling program, and a plotting program.

The control and acquisition program runs in the cyclotron control 11/34. It is responsible for running the servos for both these probes and accumulating position and current measurements every 60'th of a second when plots are being produced. The data for these plots is buffered up in designated regions in the multiport memory. Position data is run through the appropriate calibration functions before being stored in the buffer.

The data spooling program runs in the 11/45 and grabs the data buffers from the multiport memory and places it in a disk file. The spooler program then sends a message to the plotting program, which also runs in the 11/45, and tells it to read the disk buffer and plot it on a graphics terminal. The plots can later be dumped to a hardcopy device.

3.3 Monitoring And Smart Control Programs.

This is a set of programs which run in the 11/45 and either report the status of a set of devices, or control some devices in a manner not compatible with the control hardware. Space only permits a brief list of some of the programs which have been implemented in this group.

1. Control system log book generator -- This is a program which reads the control system multiport memory and produces a formatted page for inclusion in the K-500 logbook. The log book generator allows the operator to optionally include the latest set of probe traces along with the control settings.
2. Control system state saver -- This is a program which may be run to save the current control system values on a file. The file may be used later to reload the control system back to this state. This is a useful way to save optimal parameter settings for available beams.
3. Deflector Conditioner -- Conditions the electrostatic deflectors by running the voltages up at predefined rates until a current limit is exceeded, and then running the voltages back down.
4. Magnet logger -- Monitors the strain gauges, helium levels, currents and lead voltages for the K-500 cyclotron magnet (written by P. Miller).

4.0 CURRENT STATUS

At present, with the exception of the RF system, a good sample of the K-500 devices are computer controlled. In particular, the trim coils and their associated first harmonic steering bumps, as well as the extraction system. The R.F. may be turned on (warm started), the Dee voltages and relative phases may be altered or set, and pieces of the phase I beam line are also under control.

The control programs in the 11/45 add functionality which would not ordinarily be available in a hard wired control system. In particular, the plotting programs provide calibrated beam profiles at two important diagnostic regions, the system save/restore programs enable one to return reliably to a known good configuration, while the deflector conditioning program has saved many man hours of deflector conditioning by freeing the human operators from the tedious task of hand conditioning the deflectors.

A long road ahead remains however, the bulk of the K-500 R.F. system must be brought under computer control, as well as the majority of the beam lines. Work on computer control of the experimental facilities has not yet even begun, and, of course, the K-800, and coupling line loom

ahead as large systems which will require computer control.

5.0 CONCLUSIONS

The computer control system has proven useful providing, as it does, services beyond those which could be offered by hardwired analogs to the current control system. The strategy of keeping a picture of the 'state of the world' in a centrally located, multiaccess memory has greatly facilitated the development of the system by easing tremendously the communications problem typically faced by multiprocessor accelerator control systems.

THE K500 R.F. SYSTEM

J. Riedel

The K500 rf system works very well! There were some major and many minor retrofittings that had to be done to it since the first time it accelerated a beam. And, of course, there will be future upgrading as well. Still, it has performed remarkably well. Normally it works, during an experimental run, completly unattended. To change to a new frequency for a different beam requires only about 15 minutes, unless this condition requires a higher dee voltage than the previous beam, in which case perhaps another half hour is required to recondition the dees.

However it isn't perfect, and probably never will be. The initial specification called for a dee voltage of 100 KV peak. Although during initial tests we were able to achieve this, now the dee sparking limit seem to be between 80 and 90 KV. Perhaps this limit will disappear when the dees are positioned properly. Another limit, very fundamental, is sparking to the neutralizing loops in air at low frequencies. At 9 Mhz, for example, we are limited to 70 KV on the dees. Thus, certain desirable beams are unattainable. With considerable effort this problem could be resolved, for example by inserting different loops for high and low frequency runs, or by using SF_6 gas. Figure 1 shows the diagram of the major components of the rf system.

There exist two major problems with the K500 rf system: One, the dee coupling capacitor "windows" keep failing resulting in one day delay, and, two, the fingers on the stem panels burn up after a certain amount of travel, resulting in about four hours delay. We don't understand, yet, why the couplers fail, but we think we now understand why the fingers fail. It is because after a certain amount of travel the one mil gold "contips" get worn off and bare BeCu is exposed, resulting in sparking. We know how to solve this problem and will do so.

As for the couplers, we are undecided on the proper solution, but as sure as the sun will rise tomorrow we will come up with one.

Meanwhile, the rf system works quite well and has caused less down time than other systems do.

Status of the K800 R.F. system

In 1981 we had a design for the K800 rf system based on 1/2 scale model measurements of the "duck neck" dee of Resmini's design. Shortly thereafter, the dee shape was changed to a simple spiral, and because of concern over the repeated failures of the fingers on the outer conductor panels of the dee stem, a cylindrical outer conductor design was studied. Now that we believe that the K500 panel fingers will prove satisfactory by adding 1/16 inch long silver graphite contacts to the fingers we have decided to use this approach for the K800 design. We propose to go back to the 12 sided panel configuration of the 1981 design for the outer

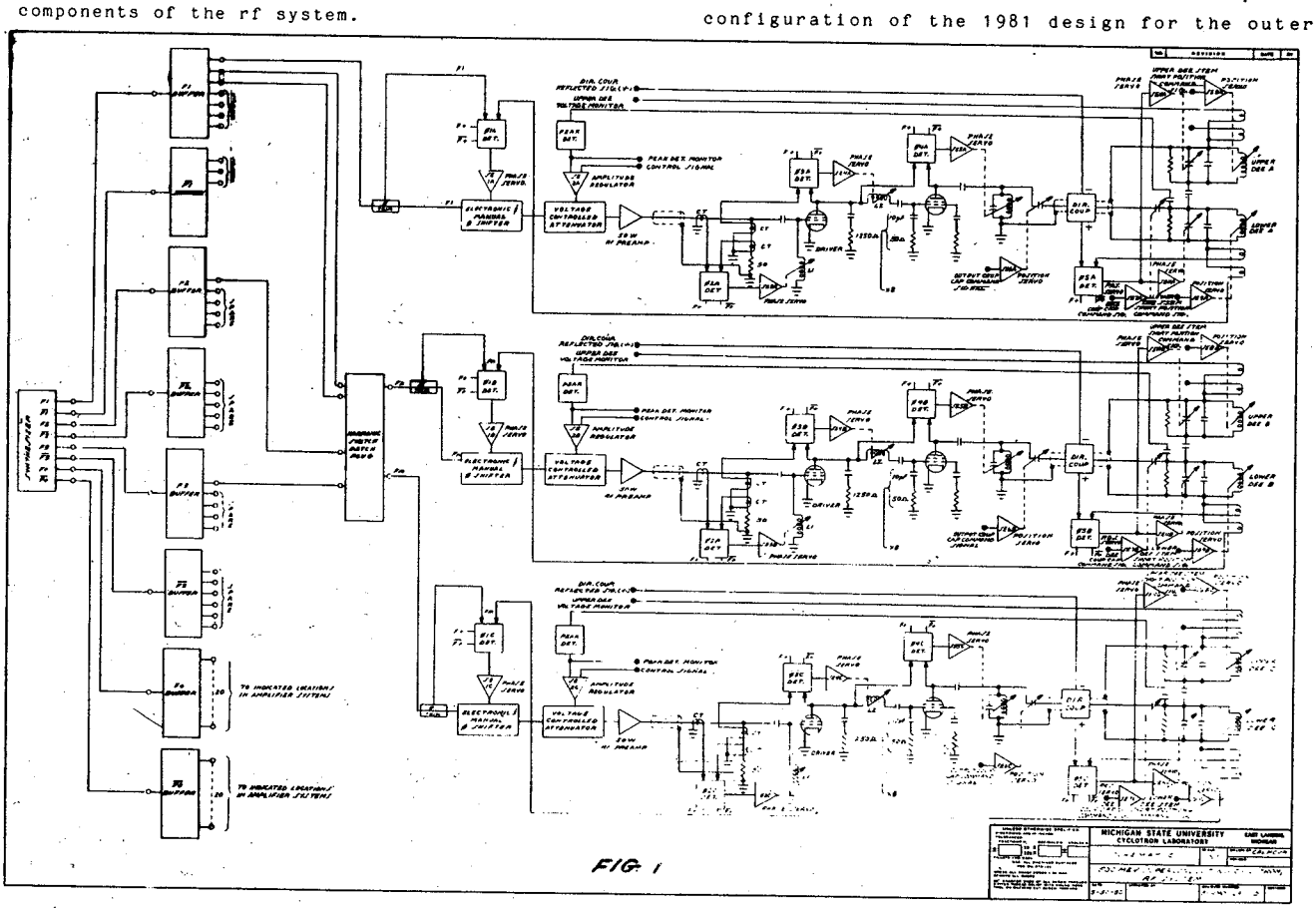

FIG. 1

conductor of the air part of the dee stem.

To achieve a top frequency of 27.5 Mhz and have appropriate room for the neutralizing loops, the detailed design of the vacuum part of the dee stem is very crucial. It is also necessary to know the electrical properties of the dee. Since these are extremly difficult to calculate we have decided to build a full scale model of the new dee plus the actual stem including the insulator and about six feet of the air side of the stem. The model will be made of wood with copper foil attached to it so that the resonance properties will be modeled precisely, though not the power requirements. This model is being designed now, and should be available for testing about 1/3/84.

Our plan, then, for the dee resonators is that it will be very similar to the K500 resonators.

A prototype transmitter is designed and all the parts are fabricated. Final assembly is now being done and it should be available for testing into the existing 300KW water load by 8/1/83. The prototype driver for this transmitter is assembled and undergoing tests now. Thus, if no modifications of the transmitter and driver are necessary, they will be finished well ahead of the resonators.

The various motor and hydraulic actuators needed will be copies of the K500 units, so no design effort will be needed for them. The low level electronics, comprising some 90 NIM modules, in 12 NIM bins will be exact copies of those used in the K500 rf system, and about 20% of these are now being constructed.

The power supplies for the drivers, the final filaments and the various screen and grids are on hand. The only power supply problem is the 1.2 MW final anode supply purchased from Aydin of Palo Alto Ca. It is on site and being tested, but various problems exist, so that it has not as yet been accepted. However, since we don't really need it for at least another year, no doubt we will be able by then to make it acceptable.

To sum up, unless unforeseen developments occur in our testing program, we should be able to have a viable rf system by the time the magnet, the vacuum system and other systems are ready for it to perform.

STATUS OF THE K500 ELECTROSTATIC DEFLECTORS

J.A. Nolen, A.F. Zeller, L.H Harwood, P. Miller, and J. Yurkon

Tests of the components of the K500 electrostatic deflectors in the K50 cyclotron and initial operation of these deflectors in the K500 cyclotron were both very promising. However, after a brief period of operation in the K500 at the design voltages of 100 kV their performance has deteriorated significantly. At the present time, with fresh insulators, the deflectors can be conditioned and operated up to voltages of approximately 70 kV. This operation is only possible while bleeding a small leak of about 0.1 cc/min of air into the high voltage feedthrough tube of each deflector. This performance also decreases with time after rebuilt deflectors are installed in the cyclotron. The degradation of performance seems to be related to accumulated insulator damage over periods of a few weeks. Conditioning of the deflectors is done with the help of a program running on the cyclotron control computer. The program can be set to raise the voltage at a specified rate as long as the leakage current is below a specified value and to lower the voltage in case of a spark or if the leakage current exceeds the specified value. Commonly used parameters are a voltage increase at a rate of 4% per second and a leakage current limit of 50 μa. If the leakage current goes above the set value the voltage is decreased by 4% per tenth second until the current drops below the set value.

Since the insulators come out discolored, spark marked, and sometimes broken after a few weeks of use in the cyclotron they are suspected to be largely responsible for the limited performance. Each deflector shoe is supported by three insulators, two in compression and one in tension. They are alumina 0.3" in diameter and about 1.2" long. We have tried metallizing the ends of the insulators and soldering metal end caps on the compressive ones to reduce insulator damage. This may have made operation slightly more reliable but the results are not very well defined due to the wide range of performance of the deflectors.

The small diameter of the voltage feedthrough tube necessitated by the small median plane penetration of the superconducting coil is also a weak point of the deflectors. It is not unusual for deflector sparks to be in this tube rather than in the actual deflector housing. The ID of the outer (grounded) tube is 1.2" while the OD of inner (HV) conductor is 0.4" leading to an electric field of 178 kV/cm at the surface of this inner conductor at the design voltage of 100 kV. We have tried both titanium and stainless steel liner tubes for this feedthrough, with stainless steel being slightly better because of its greater resistance to spark damage. Originally solid stainless steel rods were used for the inner conductor, but we are currently trying thin-walled titanium tubes in this spot. Titanium is apparently a slightly better material than stainless steel for high voltage cathodes in vacuum, and these tubes being much lighter also put significantly less vertical load on the deflector insulators. To date one of these new titanium tubes is in use in the cyclotron, but it is too early to evaluate its performance.

To more properly evaluate the significance of various small changes such as the ones mentioned above we are currently building two electrostatic test stands. In one of these it will be possible to do high voltage tests of complete deflector assemblies in a 10 kG magnetic field before using them in the cyclotron. The other is mainly for testing small components such as insulators in a more controlled environment, i.e. without all the variables of the complete deflector assembly and feedthrough. These test stands are nearly completed and will be in use soon.

Several variations on the present deflector operations will be evaluated in these test stands. Firstly, a new 100 kV power supply with an adjustable current limit has been purchased for use with these test stands and to determine the advantages of the current limiting feature. Various cleaning and polishing methods for the various deflector components will also be tried. Different conditioning procedures, leak rates, and leak gasses will be evaluated. New deflector shoes (cathodes) of titanium are currently being made in the shop. The idea of using a ceramic

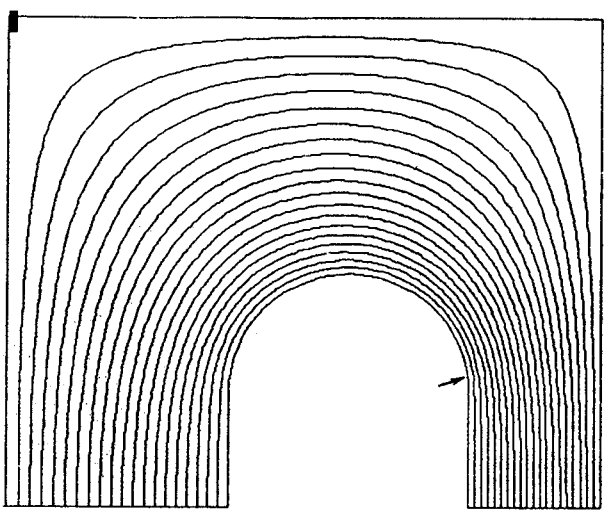

Fig. 1. Electrostatic calculation showing the equipotentials surrounding the deflector shoe with the present geometry. With a field of 140 kV/cm on the median plane, the peak field (at the arrow) is 180 kV/cm.

liner for the high voltage vacuum feedthrough has been suggested by Jack Riedel. The metallized ceramic tube is on order and will be tried in the test stand.

We have also carried out calculations of the electrostatic fields around the present shoe cross section and for the insulator end cap geometry. The equipotentials around the shoe are shown in figure 1. The shoe is 1" tall and 1/2" thick with a 1/4" radius semicircle machined on top and bottom. The design voltage of 100 kV with the 7mm gap gives the necessary extraction field of 140 kV/cm on the median plane. However, this particular shoe shape leads to a peak field of 180 kV/cm at the transition point from the straight section to the curved top and bottom. Calculations with elliptical cross sections show that this peak field can be reduced, but only at the expense of field uniformity on the median plane. Other calculations using a combination of two or more circular radii indicate that it may be possible to both decrease the peak field and improve the field uniformity with a slightly taller and slightly thicker shoe than presently being used. Fine tuning of these calculations is in progress. The calculations of the insulator end geometries, as illustrated for one case in figure 2, show that there are high fields in the recesses between the insulators and the shoe or "flower pot" end caps. This is corroborated by the observation of spark damage in these locations. There is extensive literature on the geometries of high voltages insulation in vacuum, but there is by no means a concensus of opinion on this subject. One attractive option which we plan to evaluate in the small test stand is to metallize the ceramic insulator directly to a metal button in a planar geometry. Another geometry which has been used elsewhere consists of recessing the insulator but with the metal surface joining the insulator at a finite angle.

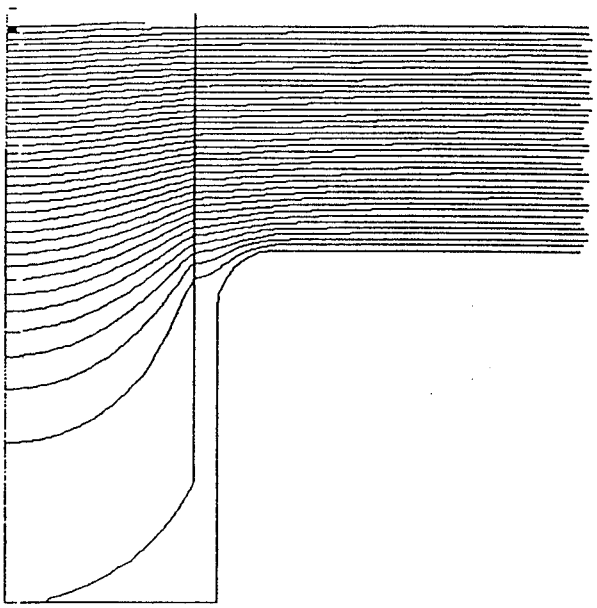

Fig. 2. Electrostatic calculations showing the equipotentials in the region of the insulator and the recess in the shoe. Insulator damage occurs around the rim of this recess.

CYCLOTRON CRYOPUMP OPERATING EXPERIENCE

P. Miller, E. Kashy, H. Laumer, M. Mallory,
and D. Poe

The pumping system for the beam chamber of the K500 cyclotron is pictured schematically in Figure 1. The three turbomolecular pumps on the top of the magnet are backed by a single rotary forepump preceeded by a liquid nitrogen cooled trap. Rough pumping from atmospheric pressure is done through the turbomolecular pumps, which are turned on when the chamber pressure is 0.5 torr. The ultimate pressure of the cycloton with this pumping system is 1×10^{-5} torr with no gas leak through the ion source. The pumping speed is conductance-limited; the three pumps together give 160 liters/sec for air, and 430 liters/sec for helium.

The cryopumps provide the large additional pumping speed needed for operation of the cyclotron. Each pump is a liquid helium cooled copper plate surrounded by a liquid nitrogen cooled box. The entire top of the box is a chevron baffle plate. The lower surface of the helium cooled plate is coated with granules of activated charcoal. The three pumps, located in the lower half of each of the three dees, are fed cryogens in series via concentric tubes in each dee stem. The interconnections are made in a junction box which feeds each pump through a removable U-tube.

The present pump heads in positions C and B have a different internal structure from the one in position A which is the prototype that was previously tested. The changes increased the thermal resistance between the liquid nitrogen and the radiation shield so that pumps B and C run at a higher temperature than A.

It is necessary to flow liquid nitrogen through the pumps at a much higher rate than the heat load demands because of this thermal resistance and the absence of any liquid reservoir in contact with the pump surfaces to be cooled. The total daily consumption of liquid nitrogen (magnet, refrigerator, and cryopumps) is about 900 gallons, of which the cryopumps are estimated to use about 600 gallons, from measurements of the liquid recovered at the exhaust. The upgrading of the B and C cryopumps and the cryodistribution lines planned for August 1983 is designed to correct these problems.

The cryopumps will have a liquid nitrogen reservoir installed in good thermal contact with the pump. The cryogen feed will be parallel flow with each pump controlled separately.

The initial development of heavy ion beams in Sept.-Nov. 1982 was plagued by recurring vacuum difficulties which were finally inferred to be the result of off-gassing of air, nitrogen or carbon

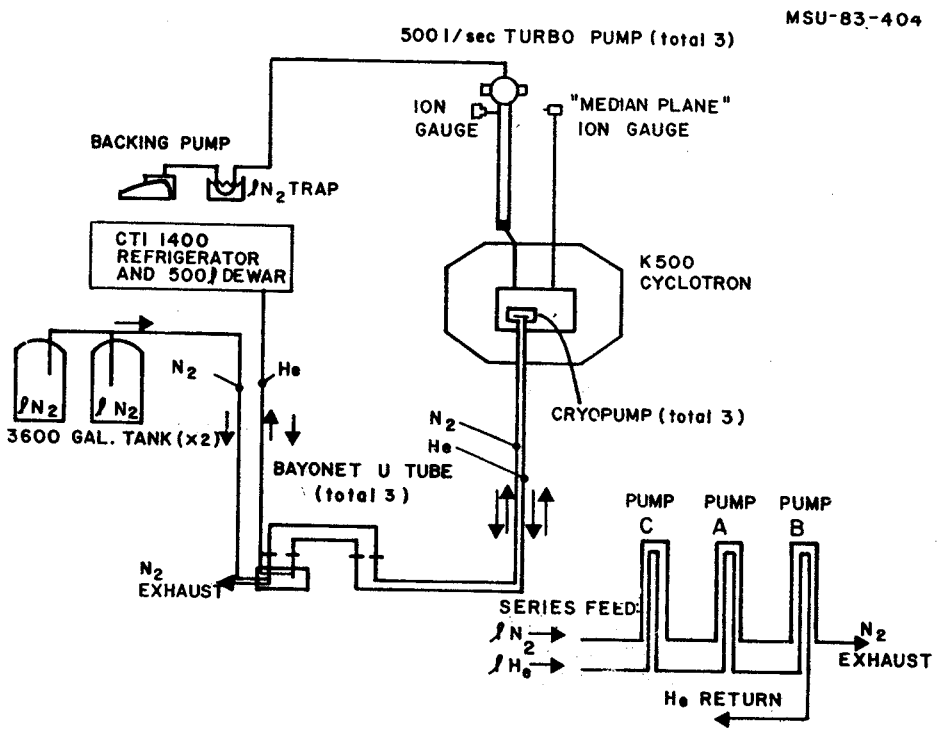

Fig. 1. Schematic drawing of pumping system for the K500 cyclotron beam chamber.

monoxide from the cryopanels due to small temperature fluctuations in the range 25K-30K. This was confirmed in December 1982 when the cyclotron was opened and thermometers were installed. At this time the charcoal was also applied to the panels. When the system was operated in the usual mode, the panel temperatures were in the above mentioned range and were controlled by the temperature of the nitrogen shields (~ 180K). Even so, the cryopanels seemed to pump air and nitrogen much better. This was attributed to the presence of charcoal. Increasing the liquid nitrogen flow to 1.5ℓ/min (the maximum possible without hardware modifications) lowered the temperatures as shown in Table 1 and allowed the use of neon in the cyclotron ion source.

The cryopanels are normally cooled for 5 days of use and then are warmed up to room temperature for two days with turbomolecular pumps running to regenerate the charcoal. When neon gas is used, the cryopanels become saturated in 3-5 days and stop pumping. This triggers an excursion of the pressure and a brief warming of the cryopanels.

The pumping speeds shown in Table 1 were measured by introducing gas at a known rate through the ion source with the arc turned off. The pressure was read with the ion gauge connected to the cyclotron through a hole in the upper pole cap and denoted as "median plane ion gauge" (See Figure 1). It is the only such gauge not located close to one of the turbomolecular pumps.

The pressure readings of this gauge were compared with pressures calculated[1] from the rate of attenuation of the internal beam current with distance from the center. There was a considerable discrepancy in some cases which may be due to the proximity of the cryopumps to the beam path (see Table 1). The pressure readings during pumping speed measurements were typically in the 2-15 x 10^{-6} torr range where the effects of out-gassing were negligible, since the base pressure reading was 2-4 x 10^{-5} torr.

1. R.A. Gough and M.L. Mallory, IEEE Trans. on Nucl. Sci. NS-26 No. 2 (1979) 2384.

Table 1. Cryopumping Data

Cryopanel Temperature:

	Pump A	Pump B	Pump C	
Typical:	10	15	15	[K]
Minimum:	7	11	11	[K]

Radiation Shield:

	Pump A	Pump B	Pump C	
Temperature (min.)	110	150	160	[K]
Uniformity ($T_{Chevron}$ - T_{box})	5	5	---	[K]
Cooldown time	8	8	8	[Hrs]

Pumping Speed (measured by "median plane" ion gauge):

CO_2	3000	[ℓ/sec]
N_2	3500	[ℓ/sec]
Ar	2500	[ℓ/sec]
Ne	2000	[ℓ/sec]
He	1100	[including 430 ℓ/sec turbos]

Capacity:

Ne	3500 STP cc @ T_A=8K, T_B=11K, T_C=300
N_2	$\geq$12000 STP cc @ 12K to 20K

Pressure in Beam Chamber during accelerator operation:

Beam	Energy (MeV/A)	"Med. plane" ion gauge Pressure (torr)	Calculated as in Ref. 1 P_{atten} (torr)	Gas
$^4He^{1+}$	25	10 x 10^{-6}	10 x 10^{-6}	N_2 (He)
$^{22}Ne^{5+}$	25	6 x 10^{-6}	2 x 10^{-6}	N_2 (He)
$^{40}Ar^{6+}$	10	6 x 10^{-6}	1 x 10^{-6}	Ar

CENTRAL REGION RADIOACTIVATION

M.L. Mallory, T. Antaya, F. Marti and P. Miller

The radioactivation of the K500 Michigan State University superconducting cyclotron central region has been detected (sec Fig. 1) and is attributed to strippd particles from the accelerated heavy ion beam. This radioactivation can pose a radiation hazard to personnel since the activated ion source is recycled after each run. Equations defining an energy band, where central region activation can occur, have been derived for a uniform magnetic field and verified by computed orbits in the actual magnetic field. Figure 2 shows the ion charge state for various atomic masses that can cause activation as a function of cyclotron size (K). The results indicate that the K500 cyclotron at Michigan State University is the first heavy ion cyclotron to operate extensively within the energy band for this process. Various options to minimize the radioactivation are;

1. Improvement in accelerator vacuum
2. Sheild the ion source with high Z material,
3. Have multiple sources and allow activation to decay,
4. The installation of an external ion source

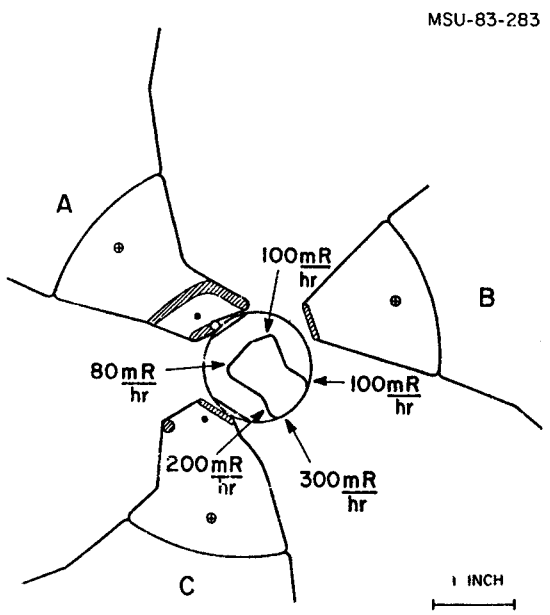

Fig. 1. The radiation measured on the cyclotron ion source is shown. The source, located between the three dees has been activated as high as 1R/hr at 3 cm.

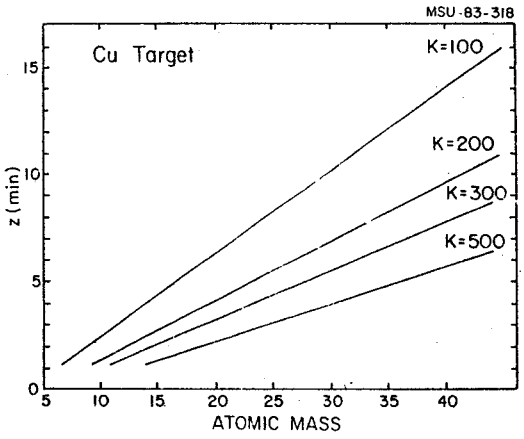

Fig. 2. The minimum charge state (z), when stripped to (Z + 1) can activate the cyclotron central region, is shown for various cyclotron K factors as a function of atomic number with copper used for the coulomb barrier.

EFFECT OF ORBIT CENTERING AND MAGNET IMPERFECTIONS ON BEAM EXTRACTION

F. Marti, H. G. Blosser and M. M. Gordon

We describe in this contribution the studies we performed to analyze the influence of the measured magnetic field imperfections on the orbit dynamics in the K500 cyclotron. We concluded from these studies that it would be helpful to shim the magnet and correct the first harmonic imperfections in the regions where ν_r=1.0.

Beam extraction is carried out by introducing a first harmonic bump in the magnetic field in the region where ν_r= 1, thereby off-centering the orbits and producing good separation between turns at the electrostatic deflector entrance. After the first few beams were extracted it became obvious that there was only a narrow range of first harmonic bumps that could be used to extract the beam, and that the amplitudes of these bumps were much larger than what we had expected from orbit calculations. The discrepancy was such that the computed orbits did not survive up to the extraction energy when the applied bumps were as large as the experimental ones.

All these computations had been done in a perfect magnetic field. The only harmonics present were the 3N harmonics and the centering coil plus extraction bump first harmonics. It was decided then to look at the magretic field measurements and work with more realistic fields in the computations. It then became clear that there were left in the machine after the measurement significant first harmonic imperfections in the extraction region (and also in the central region where ν_r= 1) which accounts for the unexpected magnitude of the extraction bump.

During the mapping process the main coil had been centered using the forces on the links that hold the cryostat tank as a guide, and the final position was a compromise between minimum or tolerable forces and first harmonic minimum.

When the measured magnetic field (including the imperfections) was used in the orbit codes the agreement with the experimental settings for the extraction bump was remarkably good, showing also the small range of angles in the extraction bump that allowed the beam to survive the vertical blow-up when traversing the $\nu_r = 2\nu_z$ resonance. We decided then to pursue a detailed study of the effect of the imperfections on the orbit dynamics and specifically on the beam extraction.

We picked two different ions to study the orbit dynamics. We considered first $^{12}C^{4+}$ 30 MeV/nucleon in a Bo = 34.5 kG field as a typical ion that we frequently run in the K500 cyclotron. The choice of the second ion was based on the ν_r behavior. We wanted to study a case where $|\nu_r - 1|$ was small and therefore possibly more sensitive to imperfections in the magnetic field. For this purpose, we studied the ion $^{40}Ar^{6+}$ 11.5 MeV/nucleon in a magnetic field with Bo = 48.2 kG (close to the bending limit in the operating diagram) and with a low charge over mass ratio (Q/A = 0.15). This ion sits in the low energy region of our first harmonic operation. For R < 10 inches, we have $|\nu_r - 1| < 0.01$.

In general, after reaching a peak near R = 23 inches, ν_r falls below 1.0, and simultaneously ν_z increases. The particles must cross two resonances in the extraction region. They are the ν_r = 1, and the $\nu_r = 2\nu_z$. The order of crossing them depends on the field level for each Q/A. The $\nu_r + 2\nu_z = 3$ resonance is beyond extraction, but we must be careful because if the beam gets to close to this resonance and is also very off-centered, the beam blows-up vertically.

One of the first calculations we made was the determination of the range of first harmonic bumps in the extraction region (produced by our trim coil number 13) which allowed us to accelerate the particle to the extraction energy without an excesive increase of the vertical height of the beam. We picked a factor of 2 growth in amplitude as the cutoff in determining whether there was vertical blow-up.

The particles were started in centered orbits approximately 150 turns before extraction (500 is the nominal total turn number for first harmonic operation). From these calculations we learned that the available area in the polar plane for the first harmonic bump had a diameter of approximately 10 Gauss centered at approximately 15 Gauss and with a phase of 270 degrees. This result explains the difficulties we had during the first extraction experiment;, that is, we had to find this small "island", or else we could not compensate the imperfections properly. Actually, this compensation can be carried out only approximately because of the difference between the form factor and phase dependence of the imperfections and the compensating trim coils.

Up to now, the K500 cyclotron has operated without no phase selection. We are in the process of designing phase slits that will limit the phase width of the beam. The central region does not establish a narrow window, allowing beams as much as 60 degrees wide to accelerate past the first few turns. With the purpose of studying the effect of phase spread, we considered ions that started at the center of the ion source slit in a ±10 degree interval around the central starting phase. This central phase was taken as 30 degrees before peak voltage between source and puller. This total of 20 degrees in phase was populated with 41 particles equally distributed every half a degree in RF time.

In comparing extraction in the case with magnetic field imperfections to the perfect field

case, we first found the amount of first harmonic from the centering coil which produced a central ray (starting time = -30 deg.) that was pretty well-centered after 150 turns.We then found the extraction bump which would allow the particles to accelerate to the extraction energy (ν_r approximately 0.8) and give good turn separation at the entrance to the electrostatic deflector. In both cases, the RF frequency was tuned to obtain minimum turn number for a starting phase close to that of the central ray.

The general behavior in both cases was very similar.The energy distribution, the time spread, and the (r, p_r) distribution at the entrance to the deflector were comparable. The case with the imperfections did not show any resultant degradation of the beam.

Each of those 41 rays that started at the ion source at different times are really "central rays" for a radial phase space area that should be accelerated. We studied the behavior of a circular phase space area in the (r,p_r) plane, corresponding to a final emittance of 7.5 mmxmrad. The result for the 30 MeV/nucleon Carbon field showed no significant deterioration of the beam when the imperfections were present. On the contrary, the 11.5 MeV/nucleon Argon field showed that the presence of imperfections opened up the ν_r=1 stop band between 1.0 and 1.5 MeV/n, and between 9.8 and 10.2 MeV/n. When the beam traverses the first of these two regions,the phase space area becomes very elongated, and as a result, when the beam traverses the second region,this area becomes extremely distorted (see figures 1 and 2). The difference in behavior here is due to the Ar field having much smaller values of $|\nu_r-1|$ than the Carbon field

This distortion will obviously make it difficult to obtain separation between successive turns at extraction, decreasing the efficiency of the extraction system. We are in the process of calculating shims that would decrease the imperfections in the regions where ν_r is close to 1.0.

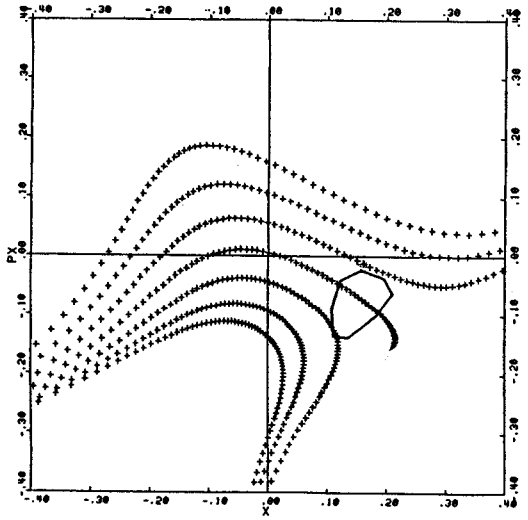

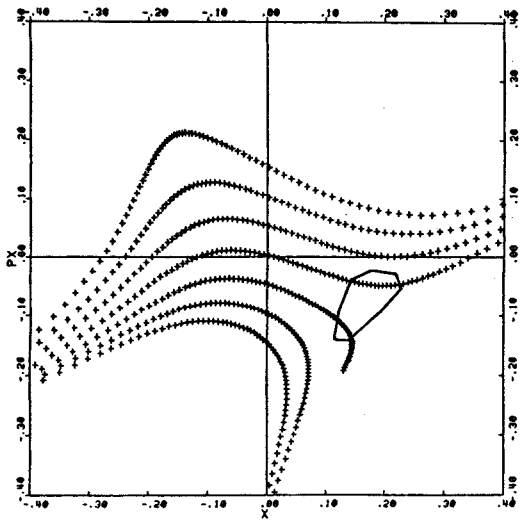

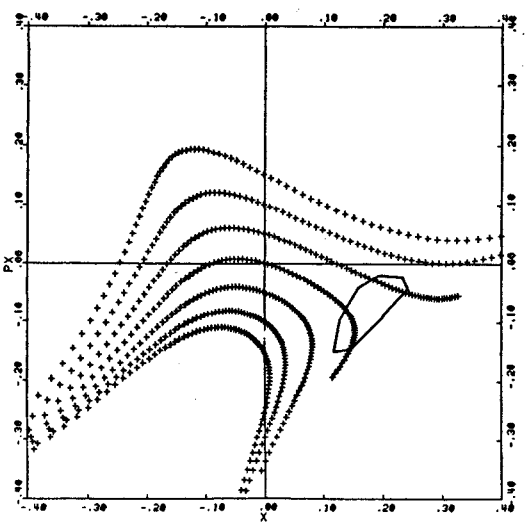

Fig. 1. Static phase space plots for the $^{40}Ar^{6+}$ 11.5 MeV/nucleon field for energies 1.26, 1.37 and 1.49 MeV/n, spanning the ν_r=1 resonance. The (x,p_x) positions are measured with respect to the equilibrium orbit in the perfect field at those energies. The polygon joins the 8 points used to define the beam in the radial plane.

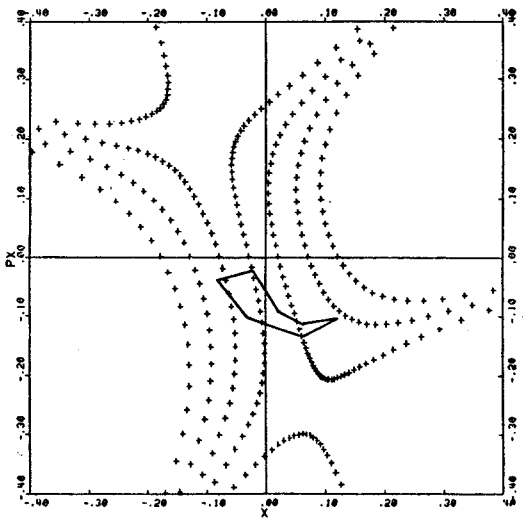

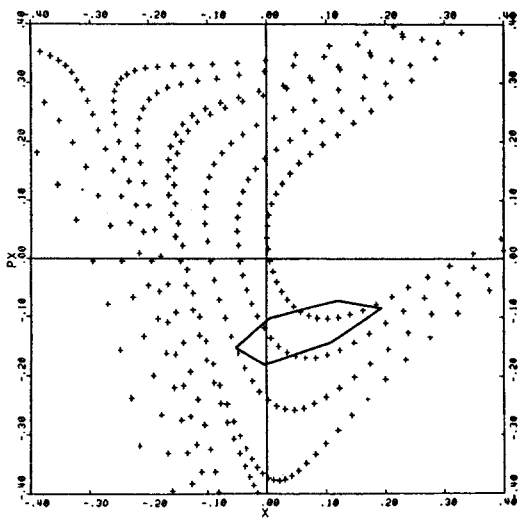

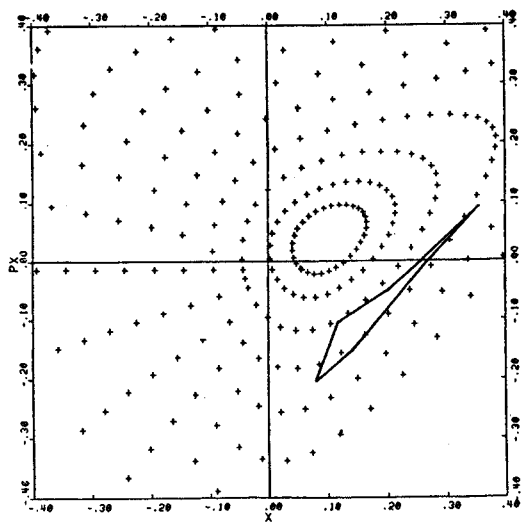

Fig. 2. Similar to Fig. 1 but for 10.04, 10.13 and 10.24 MeV/n, corresponding to the ν_r= 2 resonance near extraction.

FURTHER STUDY OF THE YOKE MAGNETIC CHANNEL IN THE K500.

Bruce Milton

In the K500 cyclotron the radial defocussing which would occur during yoke traversal is compensated by a large passive magnetic channel[1], located in the yoke. In the spring of 1983 studies of the K800 injection path[2], were restarted and during these studies it was found that a similar device would be needed for the injected beam. In order to determine the correct location and size of such a channel, a series of "poisson" calculations were performed. Much to our surprise the calculated gradients were very non-uniform over the working aperature of the chanbel (Fig. 1). This lead to a review of the

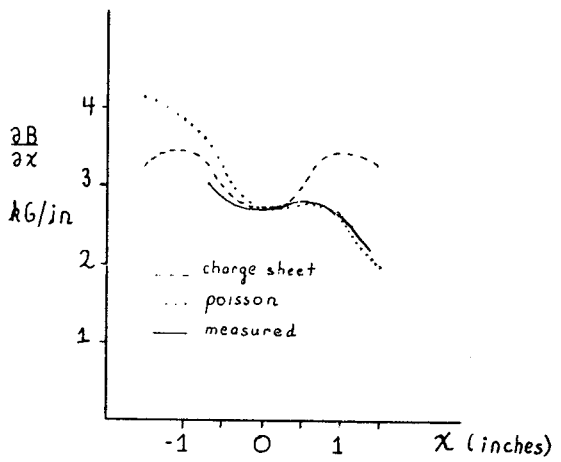

Fig. 1. The magnetic field gradient is plotted as a function of the transverse distance from the center of the channel. The charge sheet calculation yields the symmetric result reported in reference 1. Poisson calculations take into account the effects of the sides of the bars and thus should be more realistic. Measured data points are far apart so accurate gradients are not known, but it appears that they follow the non-symmetric poisson result.

measured fields in the channel region. Indeed, when analyzed, this data showed a similar non-uniformity although lack of sufficient data points leaves a large uncertainty in the gradients, particular at the sides of the channel. Immediately two questions arose: one, why hadn't this been noticed before; two, what was its effect on the external beam. It should be noted that early observations suggested that the beam was heavily defocussed in Z at the exit of the cyclotron.

In order to answer the first question, a review of the program used to convert the measured channel field data into a form usable for extraction calculations, was carried out. This program was written and used in 1980 solely by people who are no longer at the lab, so little was known about it. As it turned out the program fits the data points with a flat field and a gradient at each radius and then uses these pairs of numbers to generate the extraction field. Obviously this procedure removes any trace of non-uniform gradients, and thus all extracted beam studies have ignored the effects this may have. During this check it was found that contour plots of the old fields showed a rather "unphysical" set of equigauss curves at the entrance to the channel (Fig. 2). This is probably due to a poor procedure for matching the channel field with the main cyclotron grid.

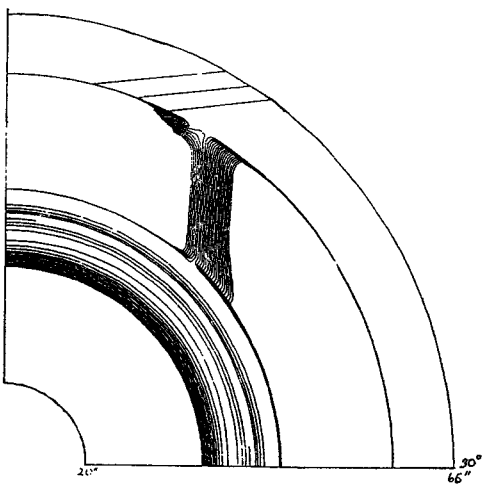

Fig. 2. Isogauss contour map of an extraction field used in the original design study. Contours are every half kilogauss from -6 kG to 6 kG.

It was felt that both of these programming simplifications could cause significant changes to predicted beam properties, so a modified code was written to provide more accurate fields for extraction calculations (Fig. 3). A set of four particles which delineate the currently used portion of the operating diagram was chosen and both a new and an old style extraction field were created for each.

Particle	Q/A	E/A (MeV)	BO (kG)
$^{40}Ar^{6+}$	.15	11.5	48.2
$^{40}Ar^{7+}$	.175	8	34.5
$^{12}C^{3+}$	.25	32	47.5
$^{4}He^{2+}$	.5	63	32.5

A comparison of the behavior of 8 radial and 4 axial phase space rays showed that the beam should be considerably more "Z" defocussed than had been previously estimated[1] (Fig. 4). At the

same time the radial phase space displays some undesirable characterestics (see figure). The new predictions would suggest that M9 is not providing the correct focusing to compensate for the fringe field, which agrees, at least partially, with current observations of the beam as it exits the yoke.

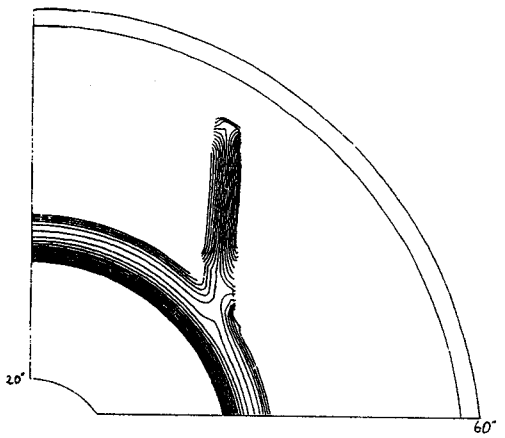

Fig. 3. Isogauss contours in a field generated by the new procedure which improves the joining of the fields. Contours are every half kilogauss.

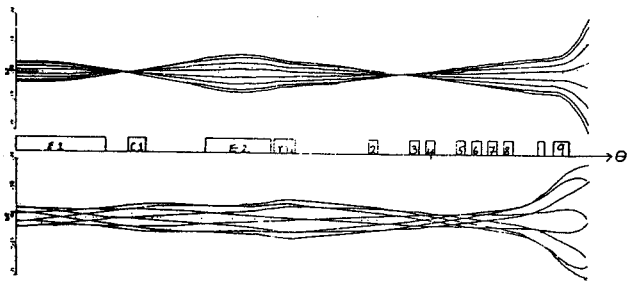

Fig. 4. 8 radial and 8 axial phase space rays tracked through the extraction system using a new field. Rays initially define an 5 mm-mrad eigen-ellipse. Note the final condition, defocussed in z and overfocussed in r.

Currently a study of possible magnetic channel rearrangements is being performed to determine if we can have a more managable beam at the entrance to M9. If that succeeds then new dimensions will be found for M9, which hopefully will reduce the axial defocussing and the radial overfoccusing (occurs in certain beams only). In order to give a high level of confidence to any such study (ie. before making modifications, the field in the channel and further in towards the coil should be remappped.

1. E. Fabrici, D. Johnson, F. Resonini, MSUCP-33.
2. F. Marti, D. Johnson, H.G. Blossar, B. Milton, Particle Accelerator Conference, 1983.

K-800 MAGNET STATUS REPORT

Lawton, Blosser, Fowler, Hilbert, Moskalik,
Morris, and Stork

Construction of the magnet components for the K-800 superconducting cyclotron is presently proceeding in many areas. Following are status and planning reports on the various activities.

Magnet steel

All major casting and surface machining operations are complete. Allignment and doweling of the magnet steel pieces has begun in the cyclotron vault. Following the allignment and doweling procedure the magnet will be disassembled for drilling of various holes in the pole caps (trim coil leads, RF system components, cryostat dowelling, etc.) and mounting of the pole tips. Drilling and allignment jigs for these operations are presently being fabricated. The main pole tip pieces have been fabricated, recieved, inspected and accepted by NSCL. Smaller details associated with the hill and valley steel shapes are in various states of design and fabrication. Major components for the upper pole cap lifting system are on order.

Trim Coils

Layout design of the trim coils is complete and tooling for the trim coil winding operation is presently being fabricated. The conductor has been received. Layout design of the potting fixture has begun. The trim coil power supplies have been received and have been installed in their permanent location.

Main Coil

At this writing the superconducting windings are 100% complete. The winding process was somewhat slowed by wire quality problems, but no major difficulties were encountered. The cryostat (vacuum vessel) for the coil is complete except for plating on the inside wall, which is part of the beam vacuum vessel. This process will be done at NSCL. Design and fabrication work for the coil support system, electrical leads, refrigeration leads, helium pressure safety system and the liquid nitrogen cooled radiation shield is presently underway. These designs are all generally upscaled versions of the K-500 designs with the exception of the support links which are planned to be composite column types with titanium tension components and a fiberglass cyclinder in compression. The major reason for changing from the K-500 design (wrapped firberglass tension links) is to save space. The main coil power supply is presently being assembled in house. Dump resistors (upscaled 500 design) are being fabricated.

Planning

Completion of the magnet steel and mail coil operations is scheduled to come together with coil testing in early 1984, followed by field mapping. (The mapping aparatus is presently in the layout design stage). Following that mapping the magnet will be disassembled for the purposes of installing the trim coils on the pole tips, and making the modifications required for the installation of the beam injection and extraction channels and the extraction hardware. We then plan a second round of magnetic field mapping in early 1985.

K-800 CRYOSTAT

H. Hilbert, G. Stork, P. Fighter, L. Gallagher,
B. Welton and B. Berning

This project started out like many others. It was the first given out as a job to the lowest bidder for forming, welding, and machining into a usable fabrication. In the process of the work it was discovered that the company could not or would not manufacture the cryostat according to NSCL drawings and specifications. Therefore it was decided to accept the parts as they were, repair what was required and complete the work in-house here at M.S.U.

First, the outer ring had to be cut, welded and re-formed so that the three outer cylinder sections could be machined from the existing stock. This work was all performed without any unusual complications.

On the other hand, the inner ring assembly was another matter. To start with, the stainless steel center ring had to be re-machined to bring it up to specifications. Then the two outer rings were rough machined and the three units were assembled on the eight foot vertical lathe and aligned.

The alignment of the three inner rings was done in a way that would allow complete clean-up of all the machined surfaces during final machining. After alignment, the three sections were tac-welded together. The alignment was rechecked and one complete bead laid in each groove. After this first weld passed, the alignment was rechecked again before the assembly was removed from the lathe for complete welding.

All the welding was performed using short welds in a predetermined pattern in order to keep the heat build-up and resulting distortions to a minimum. A 310 sst rod was used throughout the stainless to steel welding in order to insure as straight as possible a magnetic line at the steel to stainless steel interface. After each complete pass, the weld area was ground smooth and dye-penetrant checked for holes or cracks. When such inclusions were found they were ground out and repaired before any further welding was started.

After welding the inner cylinder assembly was again aligned on the lathe and machining started. After each cut, a reading was taken and plots were made using polar coordinates in order to know the amount the cylinder distorted as metal was removed and the built in stresses relieved. This movement was so great that the top and bottom flanges were installed to form a more rigid structure before the final cuts were made.

The graph shows that the welding and machining procedures produced a wall thickness that did not vary over .002 inch and a roundness within .006 inch.

When the machining was complete, the parts were blanked off and the assembled cryostat leak checked. No leakes were found in any of the welds. The next operation was to nickel plate the inside wall and part of the flanges in order to make these areas corrosion resistance and improve the outgassing rate at ultra high vacuum.

MSU-83-415

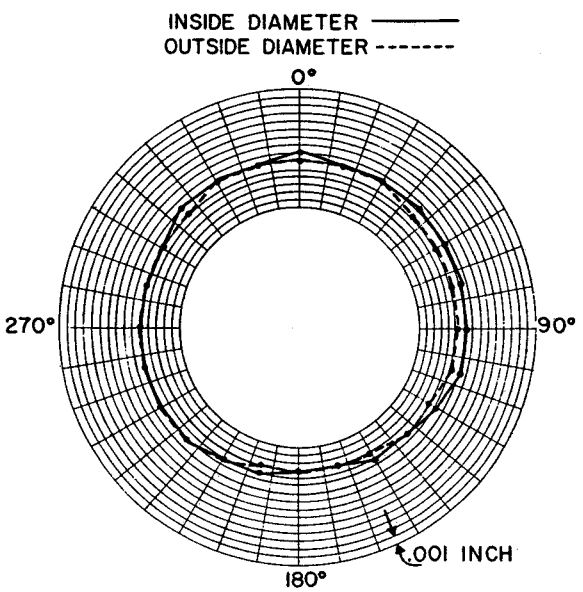

K 800 BOBBIN
LOWER CYLINDER
ROUNDNESS & WALL THICKNESS VARIATION

MSU-83-416

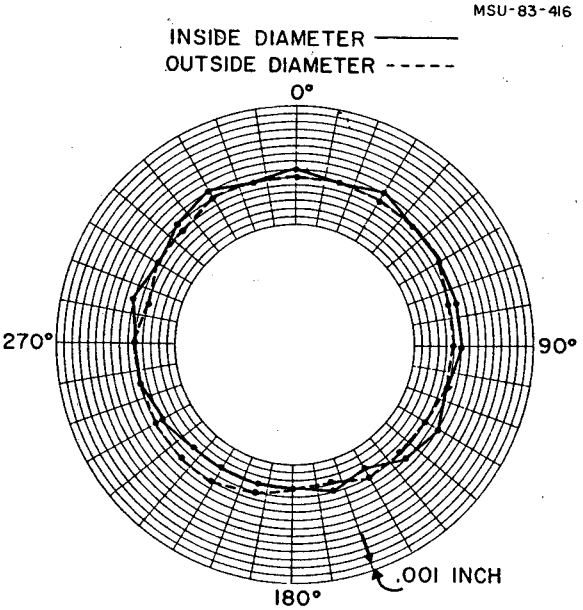

K 800 BOBBIN
LOWER CYLINDER
ROUNDNESS & WALL THICKNESS VARIATION

HIGH BRIGHTNESS ION SOURCE FOR DIRECT BEAMLINE ANALYSIS

D. Mikolas and J.A. Nolen

A high brightness, extremely small phase space ion source is being built for beamline diagnostics. Ion energy can be varied from 0-100 keV, which translates to a rigity of 0.6 Tesla-meters for a 100 keV gold beam. Most ions are emitted with a charge of +1, but molecules of two atoms with a total charge of +1 are possible if higher rigidities are desired.

The spot size is less than 100 Å. With suitable apertures and focusing, 100 nA can be delivered into a 1 mm diameter beam with a divergence of 10^{-2}mr, and 1 nA at 10^{-3}mr. Energy spread is less than 10 eV[1].

The source consists of a hot tungsten needle with the metal to be ionized plated onto the tip. The needle is biased positive relative to an extraction grid a few cm away, biased at an intermediate positive potential. A second grounded acceleration grid is placed a few cm after the first.

The metal migrates, or flows under electrostatic forces (depending on the temperature of the needle and thickness of the plating) to the tip of the needle, where the field is as high as a few V/Å. This field is sufficient to remove the least bound electron from the atom, allowing the ion to escape the surface and accelerate. Since all ionizations occur on a conducting surface at a fixed potential, a very low energy spread is expected. Typical results from energy spread measurements from sources of this type range between 2-8 eV, depending on the type of materials and voltages used.

So far, a test stand has been set up, and some measurements have been made. Gold is electroplated on to a small tungsten needle, which has been electrochemically etched to a point in NaOH[2]. The needle is spot-welded to a tungsten filament that dissipates~10W at the melting point of gold.

Beams of 1μA have been sustained for 45 minutes, and 10μA for a few minutes. Current depends roughly on the square root of extraction voltage in the range of 1-30 kV. Ion current is extremely sensitive to temperature; it doubles for a 5% change in the heater filament current (around 6A at 1.5V).

---

1. B.M. Schwarzschild, Physics Today July,1982 p.20.
2. Suggested by C.P. Browne, Notre Dame University, private communication.

STATUS OF THE K500-K800 COUPLING LINE

L.H. Harwood, J.A. Nolen, and H.G. Blosser

Since the last report, the optical design of the coupling line has not changed significantly. Most of the effort has gone into hardware considerations. The principle optical change has been in the injection section of the beamline, ie. that part after the achromatic double-waist; it has been redesigned for simpler tuning from that shown in the figure in last year's annual report. At the present time there is some concern over compatibility of the design for the first 5 meters of the beamline and the nominal trajectory of the beam. During the initial running period of the K500, it was found necessary to add two small dipoles to the beamline in the first 5 m outside the cyclotron which were not envisioned in the design calculations; the purpose of these magnets was to counter the deflection of the beam by the large fringe field of the cyclotron. The positions of these dipoles overlap with the four quadrupoles which match the beam into the acceptance of the coupling line. Presently under consideration are a change in the nominal beam direction, to more closely parallel an "unsteered" beam, and the addition of iron shielding to reduce the flux in the beam area. If the shielding works, then no major change will be needed in the optical design. If it is not successful, then at least one additional dipole will have to be accomodated in the first 5 m of the coupling line; the density of magnets is sufficiently high in this area that such an addition would not be trivial. However, a viable solution would be to use shorter quadrupoles (effective length less than 0.4 m) in this region and thereby generate the necessary space. The dipole which would be added could be made superconducting and included in the cryostat which would house the four quadrupoles. We therefore conclude that the fringe field will only slightly alter the present design.

Design on the magnets for the coupling line is proceeding. The large 135 degree magnet will probably resemble the +/- 16 degree switching magnet design, in cross section. This design has very good field quality, and the construction of its prototype should begin soon. The coil will be potted and use low current (< 200 A) conductor. The dipole which will switch the beam into the coupling line is as yet somewhat of a question. It needs a relatively high field (17.5 kG), and also needs to let the beam bend 35 degrees or go straight. The initial attempts at producing a satisfacory "C" magnet were unsuccessful. The field level needed seems incompatible with a reasonably sized "C" magnet. Currently under consideration are "H" magnets with a removeable side yoke and one with a hole bored in the outer yoke to let the beam exit.

CRYOSYSTEM STATUS

M.L. Mallory, H. Laumer, and A. Gavalya

The following sections are a summary of progress with various cryogenic systems during the past year and previous annual reports should be referred to for additional information.

CTI-1400 Refrigerator Operating Experience

The 1400 refrigerator is presently connected to the K500 cyclotron and, during the last year, the program required its continuous operation. Problems and maintenance of the 1400 had minimal impact on the K500 operation schedule since most problems were solved during the failure of other cyclotron components. The following major problems were encountered and solved.

A. Heat Exchanger Water Leak

The 1st stage after cooler (helium - oil to water heat exchanger) of one compressor unit developed a water leak. The initial symptoms were detected in the 1400 coldbox and are the following. The liquid helium production decreased with time and within one week was unable to keep up with the K500 load. Warming the high temperature end of the cold box, where water would be expected to freeze out, restored the refrigerator to its maximum performance. Finally loss of oil from the offending compressor was traced to a broken silver solder joint in the heat exchanger. We are presently installing water sensors which will facilitate monitoring He streams for this contaminant.

B. Compressor Control Wiring Short

An intermittent electrical short in the compressor protective circuit was encountered; it would blow the 1400 control fuse, thereby stopping the 1400 compressors and causing gas to vent. The intermittent short was finally made permanent by increasing the fuse rating, which put more power thru the short and fused it to ground. It was traced to a control wire that was draped over a sharp metal edge, which, after six years of vibrating, had pierced the wire insulation.

C. Interconnections of 1400 and K800 Refrigerator

The K800 refrigerator dewar was connected to the K500 dewar to be able to supplement the CTI-1400 by transferring liquid helium. As to be expected, the boiloff during transfer, which came back through the return heat exchanger of the coldbox, led to thermal (mass flow) mismatch of the 1400. However, this did not affect operation of the K500 cyclotron. A warm temperature line valved in the transfer line between dewars successfully allowed line cooldown and avoided the warm line heat pulse. A transfer of ~400l of liquid helium could be done in 6 hours. Finally, the K800 compressor (~60 g/sec) was connected in parallel with the three 1400 compressors (~13.7 g/sec). This easily increased the performance of the 1400 coldbox and allowed the off line maintenance of the 1400 compressors. Use of the K800 compressors when transferring liquid helium between dewars also allowed mass flow matching in the 1400 coldbox and one could transfer 400l in ~3 hours. Bringing the K800 compressor on line, had to be done with care since the compressors could lower the pump suction pressure and thereby flash the liquid helium on top of the K500 magnet below the desired operating point.

D. Lead Flow Experiment

When the K-500 is energized, lead gas flow is adjusted by hand operated metering valves to insure proper cooling for the particular current flowing in the leads. Should all compressors fail, as during a power failure, then the suction pressure rises to 3.5 psig whereupon boil off gas vents through a popoff valve. Since lead gas flow will diminish under these conditions, a solenoid actuated bypass valve, which opens when compressor control power is lost, is in parallel with each hand valve. In a test it was observed that upon compressor shutdown the lead gas flow diminished by a factor of ten within one minute of cutoff. The solenoid bypass valves are thus needed and insure adequate flow during the magnet rampdown procedure.

K800 Temporary Cryogen Supply Lines

When the K800 coil is ready to be tested, liquid nitrogen and helium supply lines will be needed. While a general cryogen distribution system is planned for operating the combined cyclotrons, beamline, and spectrograph magnets, a set of temporary lines from the W-800 refrigerator-liquefier and its associated dewar will supply the refrigeration for testing the K800 coil. Most of the ambient temperature return gas piping is installed. The temporary cryogen transfer lines are designed and parts are being procured. The interesting feature, which is a departure from our past cryoline designs, is that the pipes which carry cryogenic fluids will be made of Invar-36. The advantage of Invar is that its thermal expansion is small. A tube cooled from room temperature to liquid nitrogen temperature will experience a contraction about 1/7 that of 304 stainless steel. The stresses occasioned by temperature changes are then much reduced and simplified designs are then possible. Extensive use of Invar piping in the general cryogen distribution system is planned and the temporary lines will be a good test; the longest line will span 65 ft.

To check the characteristics and performance of an Invar pipe sample, a few tests were carried out. A four foot tube sample was available. Dimensions in inches were 1.3125+ 0.0006 average O.D. and 1.1725+ 0.001 average I.D.; variations in I.D. dimension were more pronounced especially at

the tube weld joint. A 2 ft section was prepared for a thermal expansion measurement. Thermocouples were attached, soldered 1" from ends and at the center of the tube. The assembly was wrapped with pipe insulating foam and immersed in liquid nitrogen. When temperatures had stabilized, the assembly was lifted out of the liquid and the expansion was measured by monitoring a dial indicator reading vs. the change in temperature determined by the thermocouples. Three trials were performed. The ratio {L(273K)-L(90K)}/L(293K) was determined to be $(3.5+0.3)*10^{-4}$. A systematic error of 15% introduced by changes of temperature of the dial indicator stem is possible.

To test the tensile strength of the Invar-36 sample, a 10 in. long tube section was prepared. A length of 2 inches was turned down to a diameter of 1.2425+ 0.0015; the wall thickness was then 0.035 + 0.002. End caps with tangs were machined from stainless steel and were welded to the tube. The assembly was mounted between the jaws of a tensile strength testing machine. A cup surrounding the reduced section was filled with liquid nitrogen and after all intense boiling had subsided the tensile strength test was performed. the sample failed at a stress of $1.40*10^5$ psi. The elongation of the reduced section was measured to be (26.8 + 0.3)%. Table 1 summarizes the measured properties and compares them to data from other sources.

Table 1.

Property	Tube Test Sample	Literature
Thermal expansion {L(273K)-L(90K)}/L(273K)	$(3.5 + 0.3)*10^{-4}$	$3*10^{-4}$
Tensil Strength at 77K (in psi)	$(1.40+0.03)*10^5$	$1.56*10^5$
Elongation at 77K	(26.8 + 0.8) %	26.6 %

A crude embrittlement test at 77K was also performed. A 4 in. long tube sample was immersed in liquid nitrogen. Once all boiling had stopped the sample was removed and struck hammer blows. The sample deformed but did not crack.

The conclusion to be drawn from these tests is that Invar-36 should be a desirable material for cryogenic transfer lines.

K800 cryoline studies

Fig. 1. is a physical layout of the continuous flow liquid helium distribution system for Phase II of the project. It consist of a main distribution system that operates full time and 12 branches that can be easily turned on or off. The 12 branches are each separately operating beam lines. Fig. 2 is a detailed valve drawing of the main branch and is closely modeled after the successfully operating K500 prototype. Fig. 3 shows a branch connection at one of the dipoles. An all welded system is planned. The continuous

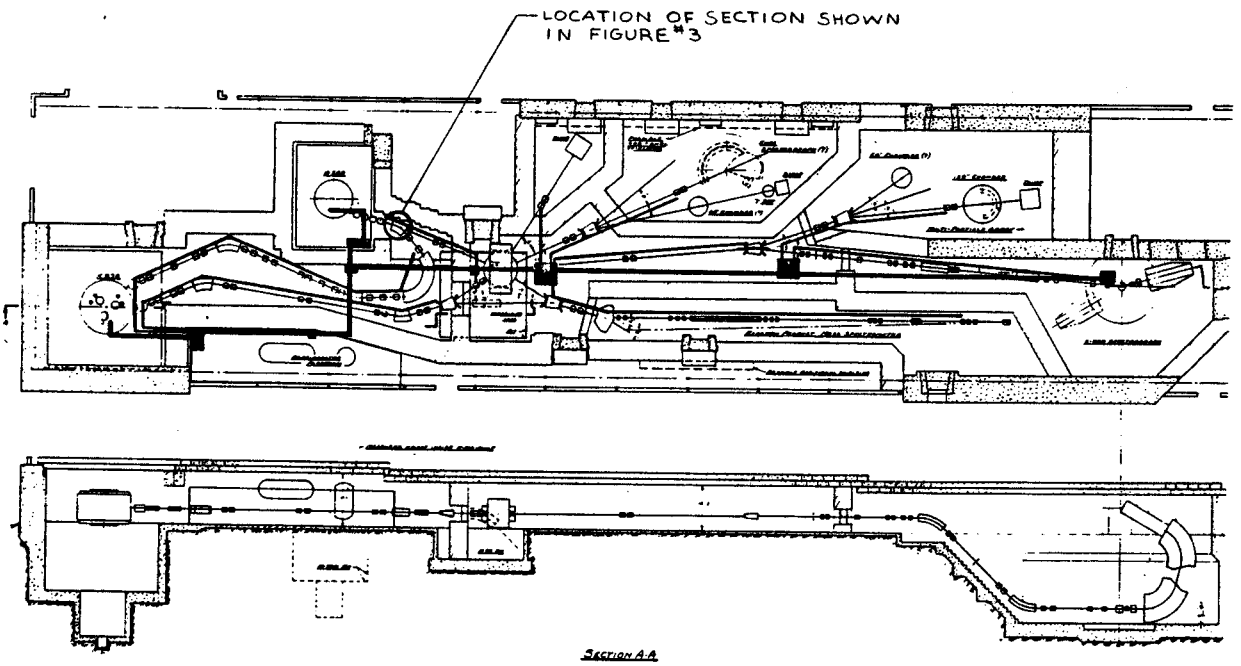

Fig. 1. The proposed beamline system for the Phase II project is shown with the cryodistribution system overlaid. The broad dark lines are the main line, and the narrow lines are branches.

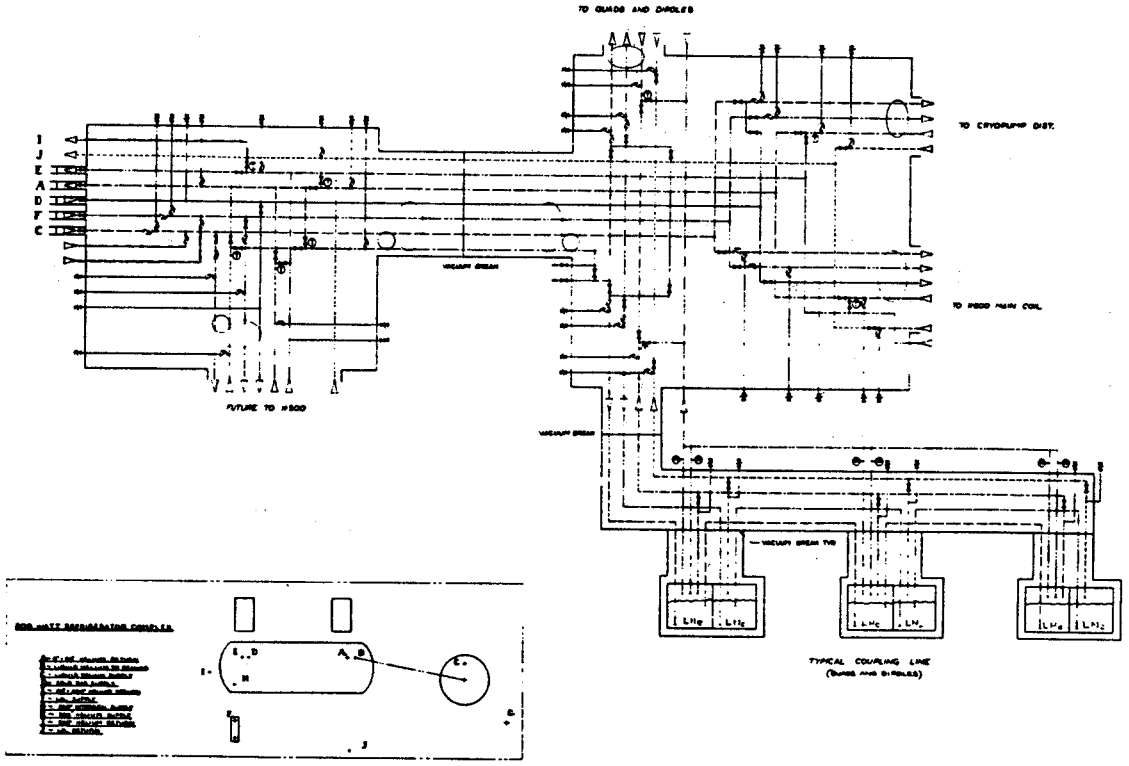

Fig. 2. The detailed piping diagram is shown for delivery of cryogens to the K800 and K500 and a typical branch.

flow system is expected to require little attention except during transient modes such as cooldown.

K500 Cryopanel Operation

The cryopanel design has been reported previously and tests on pumping speed and performance of the cryopanels are noted in another section of this report. The operation of the cryopanels has become routine, however, a number of unforeseen quirks in the behavior of the system has led us to schedule a reworking of the cold head that brings cooling to the nitrogen shields on two of the panels. This note addresses the cryogenic operation of the panels in the past year.

The standard procedure to put cryopanels in service starting from room temperature is as follows. The liquid flow to the nitrogen cooled shields is initiated first. Ater four hours the shields are close to their equilibrium temperature, at this time cold helium gas from the CTI-1400 refrigerator is allowed to circulate through the helium cryopanel passage. The panels are cooled to ~30K by the gas in three hours at which point liquid feed is initiated. In about 10 minutes the panels then reach their equilibrium operating temperature between 8K and 25K. This temperature depends mostly on the temperature of the surrounding liquid nitrogen cooled shield. About 30 l of liquid helium inventory are used up in the described cooldown procedure. The step using helium gas cooling can be skipped in which case the panels are cooled to operating temperatures in 70 minutes, but liquid consumption rises to 80 l. Finally liquid helium cooling can be initiated before the shields are completely cold. The minimum complete cooldown time from room temperature to cryopumping temperature is then four hours; the limiting factor is the cooldown time of the shields. The liquid helium consumption for this cooldown mode is over 100 l.

The combined refrigeration load of coil and cryopanels is less than 85 watt. When the CTI-1400 refrigerator-liquifier is operating well, it supplies this refrigeration and registers a dewar liquid rate of rise of 5 l/hr. As contaminants build up in the refrigerator, liquid from the dewar is used to supplement the refrigerator output. The performance of the cryopanels is not influenced by slow degradation of refrigerator performance. As noted above, the CTI-1400 system can receive liquid transfers from the K-800 system so that disruption due to low liquid helium inventory has become rare.

The temperature of the liquid nitrogen cooled shields dominate the performance of the helium cooled cryopanels. There are three panels A,B, and C. Due to variations in design, the equilibrium temperature of the shield on A can be as low as 110 K while B and C, which are

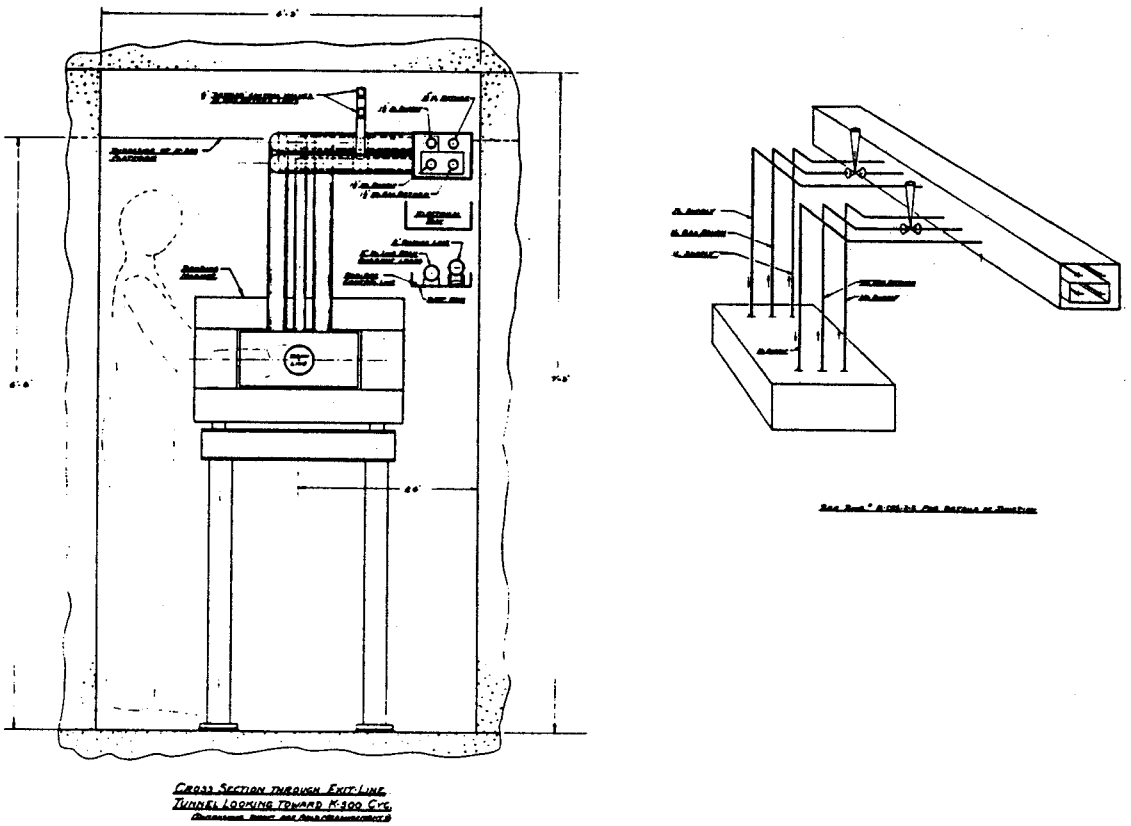

Fig. 3. A drawing showing a proposed connection scheme along a beam line.

identical, never cool much below 160 K. Liquid nitrogen flow proceeds from C to A to B and then is exhausted to atmosphere. Usually the C shield shows the warmest temperature. It was found that to cool all shields sufficiently an excess of liquid nitrogen flow at the rate of 0.5 l/min, measured at the exhaust port, had to be established. The liquid nitrogen is supplied from dual storage tanks. Tank pressure can vary from 25 to 40 psig. Bulk liquid temperature is usually at the saturation temperature except during a few hours after a tanker truck has just refilled the tanks. The introduction of subcooled liquid changes the flow through the system such that C shield warms a few degees. This result is somewhat surprising. Only limited information about the state of the cryogenic fluid is available. The liquid enters the building in a vacuum superinsulated line. A nitrogen gas filled vapor pressure bulb samples liquid temperature and a pressure tap gives the line pressure at that point. The fluid finally delivered to the cryopanels first flows through other nitrogen cooled shields about the transfer line and valve intercepts. The fluid pressure is measured between C and A as well as between A and B cryopanels. No information about fluid quality is available at these points.

The observations are summarized in table 2 and 3. Table 2 shows that cryopanel pressures are about 10 psi higher and pressure oscillations are more damped when subcooled liquid enters the line. Table 3 gives the history of cryopanel shield temperature during and following the liquid nitrogen delivery of 8/9/83. It is atypical in that A shield temperature is relatively high to start out but it does present the effect observed very clearly. It shows that cryopanel shield C, which receives the liquid first, actually warms up during and a few hours after a liquid nitrogen delivery, while A and B may be cooling down during this same time. Column 5 shows the usual status before delivery; the status shown in column 3 would then be observed after delivery. The change of temperature of C shield can be in part due to the higher saturation temperature as the pressure rises and it can be caused by the changes in flow characteristics as the gas volume fraction decreases. Since the geometry of the cold head for the nitrogen shield is rather complicated, it is difficult to make a model for calculation and to account for the observed result that the C shield gets warmer.

In summary the cryopanels have routinely operated successfuly but two problems remain to be solved. Excess liquid nitrogen consumption must

be reduced and the shields should become less sensitive to the quality of the fluid delivered. Design modifications addressing these problems are underway.

Table 2. Pressure variations observed.

	When Liquid is at Saturation Temperature			When Liquid is Subcooled	
P1	30	30	30	21	21
P2	28	28	28	34	34
P3	12.8	16	13	28	26.5
P4	6.5	10.5	7.5	15	15.5
Time (min)	0	2	6	0	1

P1 is the pressure in a nitrogen vapor pressure bulb.
P2 is the line pressure at the location of P1.
P3 is the pressure between C and A shield.
P4 is the pressure between A and B shield.
Time gives an indication of the oscillation frequency.

Table 3.
Cryopanel shield temperature history for the delivery 8/9/83. Temperatures are in K.

	1	2	3	4	5
C	173	179	182	163	171
A	170	122	116	112	118
B	176	176	162	151	163

1. Status before delivery. In this case tank level and pressure were low so even shield A was at a rather high temperature. This is a marginal operating condition for the cryopanels.
2. Status just after delivery.
3. Status 2 hours after delivery.
4. Status 20 hours after delivery.
5. A typical operating condition, often the starting point when a liquid nitrogen delivery is made.

Operation of the K-800 Refrigerator-Liquifier

As noted in the 1981-1982 Annual Report the K-800 refrigerator-liquifier was producing liquid at the rate of 100 l/hr in July of 1982. The acceptance test specifications call for a 100 l/hr rate of rise of liquid level in the dewar while simultaneously 400 watt of refrigeration at 4.5 K must be provided. In July of 1982 the major reason why this performance could not be achieved was perceived to be the limitation imposed by the compressors which functioned at ~ 50% of the design value. It was discovered that the first and second stage of the compressors were not well matched; a change to a second stage with a more appropriate compression ratio improved the performance of the combination considerably. However, the measured mass flow still falls short of the design specification. An experiment in which the Sullair screw compressors were supplemented with the flow capacity of the three CTI-1400 compressors did show that a significant gain can be expected by upgrading compressors.

Table 4 shows a history of the performance of the system as hardware changes have been made. Between July, 1982, and the data entries of 12/8/82, the compressors had been matched and an improved type of piston had been installed in the expansion engines.

To simulate a heat load at 4.5 K, a resistance type heater is operated immersed in liquid helium in the receiving dewar. There is some evidence that the refrigeration power of the plant measured by this means depends on dewar transfer line geometry. This line is a coaxial structure with the central tube transfering two phase fluid to the dewar and the gas being returned in the annular space surrounding it. Incorporating a temporary 1 ft extension in the feed line yielded a dramatic improvement in the measured refrigeration power (12/21/82). It was determined that the transfer line did not reach through the bayonet guide sheath in the dewar neck. To reduce any heat load due to this design error the transfer line was modified by lengthening it 1 ft. No improvement in liquid production was noted and there is some evidence that the refrigeration achieved is below that of the 12/21/82 test.

Table 4.

Date	Liquifaction (g/s)	Heater Power (watt)	Trial Length (hrs)	Comments
12/ 8/82	4.3 -0.2	0	1.78	
12/10/82	1.3 -0.1	200	1.85	
12/10/82	0.0 -0.3	250	0.95	
12/21/82	0.3 -0.2	380	1.35	1
12/21/82	0.6 -0.4	450	0.67	1
12/21/82	4.2 -0.2	0	1.53	1
1/11/83	4.4 -0.1	0	1.83	2
1/14/83	1.1 -0.1	300	4.32	
3/23/83	4.6 -0.3	0	0.85	
3/31/83	4.2 -0.2	0	1.30	
4/21/83	4.6 -0.2	0	1.43	
6/ 8/83	4.1 -0.2	0	1.27	
7/26/83	4.7 -0.4	0	0.58	
7/26/83	5.4 -0.2	0	1.17	
7/27/83	1.8 -0.1	400	2.07	3
8/16/83	6.2 -0.1	0	1.13	3
8/16/83	0.3 -0.1	510	1.72	3
8/17/83	4.12-0.03	0	2.68	3
Acceptance Specs.	2.79	400		

1. A temporary 1 ft. tube extension was fitted to the delivery line of the transfer line during this run.
2. The transfer line was lengthened by 1 ft. to get dewar gas return inlet out of the bayonet sheath.
3. The three CTI-1400 compressors adding a nominal total of 13 g/s were operated in parallel with the Sullair compressors.

The addition of the three CTI-1400 compressors improved liquid production by ~20%. Between 7/27/83 and 8/16/83 a high pressure seal in the expansion engines was modified to reduce blowby. During the test following this modification a production rate equivalent to 187 l/hr was achieved. The refrigeration power measured during this test period was less than 575 watt but greater than 512 watt. The question remains whether upgrading compressors alone will bring the system to comply with acceptance specifications. Modifying the transfer line to the dewar is indicated as a possible next step.

The Sullair compressors have now been operated for over 1000 hr. The only equipment failure experienced to date was due to a shaft seal that repeatedly leaked oil. The malfunction was traced to high copper content in the compressor oil; the copper plated out on a sealing surface, destroying the finish and causing the

seal to leak. Replacing the compressor oil has alleviated this problem.

Since the compressor oil used in these machines must be degassed and be free of water, a processing unit has been put in service. It consists of a 90 gallon capacity tank which can be pumped by a roughing pump through a liquid nitrogen trap. A heater elevates the oil temperature to speed the decontamination process.

A hydraulic pump and liquid transfer manifold has also been installed. Oil can now be added to compressors while they are running. The pump is also used to stirr oil while being processed and it generally facilitates all oil transfer operations.

A number of problems of the new refrigerator-liquefier became apparent and have been addressed in the past year. The system has already been used on occasion to provide liquid for the circuit usually serviced by the CTI-1400 plant. Even though the system does not meet design specifications at this time, the capacity achieved to date should easily satisfy the needs of the lab for a number of years.

A Cost Analysis of the Liquid Nitrogen Supply for NSCL

As the K-500 cyclotron has come on line the consumption of liquid nitrogen (LIN) has increased considerably. The peak usage for a 24 hr period in the last year was near 2500 gal/day. The average consumption for the last 6 months was near 1000 gal/day. The main devices using LIN to date are the CTI-1400 refrigerator-liquifier, the K-500 cryopanels, the K-800 refrigerator-liquifier, and cryoline shields including the magnet coil shield. LIN is also consumed filling detector cryostats and supplying the lab with dry nitrogen gas. A planned upgrading of the cryopanel shields is expected to reduce their consumption; however, as the tests of the K-800 coil get underway the K-800 refrigerator will be running more frequently. The rate, when all equipment needed for operating the K-500 cyclotron is being supplied with LIN, will be at the 2000 gal/day level. As the K-800 cyclotron and auxillary proposed equipment such as superconducting beamlines and spectrograph magnets come on line, the LIN use level will further increase.

An estimate for requirements of a system utilizing 800 watt of 4.5 K refrigeration may start with information from the present system The nominally 95 watt at 4.5 K refrigeration provided by the CTI-1400 generates the need for from 300 to 500 gal/day of LIN in addition to the refrigerator requirements. The combined K-500 and K-800 system must be expected to require more than 3000 gal/day.

Presently LIN is bought by the trailer load and delivered into two 3600 gal. dewars. The liquid is withdrawn on demand; the dewars are pressurized to between 30 and 40 psig. The alternative under investigation is a nitrogen reliquefier operated much the same as the helium refrigerators are operated now.

Table 5.

Refrigerator (Capacity l/hr)	Refrigeration W/W (A)	Liquid Production W/W (B)	Power cost c/l (C)
Ideal He cycle	70	326	1.1
(D) He(12)	830	6100	18
(E) He(180)	380	1900	5.8
Ideal N_2 cycle	2.9	3.9	0.8
(F) N(468)	13		2.6 (G)
(H) N(88)		22	4.5
(H) N(328)		19	3.8
(H) N(1050)		16	3.3

A. In this mode vapor is returned to reliquifier at saturation temperature. Listed is watt of power required per watt of refrigeration.
B. In this mode vapor is returned warm to compressor. Refrigeration is achieved by vaporizing liquid and the gas sensible heat is lost to the cycle. Listed is watt of power required per watt of refrigeration.
C. Power cost in cents per liter cryogen produced is listed based on 4.5c/kw hr.
D. Based on nominal performance of a CTI-1400 without liquid nitrogen precooling.
E. Based on achieved performance of in house equipment. Operated with liquid nitrogen precooling; the power cost to produce the liquid nitrogen consumed is accounted for.
F. This represents a system running in a mixed mode with 50% of the mass vaporized returning warm and the remainder at saturation temperature of the liquid. It is the model on which the cost analysis for aquiring a reliquifier is based.
G. The present cost of delivered LIN is 5.9 c/l.
H. These table entrys represent commercial reliquifiers and are listed to give an indication how efficiency improves with increasing capacity.

Table 5 presents a summary of power costs of interest in operating helium and nitrogen refrigerators. It is apparent that while the power cost is a small fraction of the commercial cost for liquid helium, it is a significant fraction of the cost of LIN delivered by truck. This implies that only an efficiently operating reliquifier can compete with commercial liquid nitrogen deliveries.

Based on a recent quote a 10 ton/day reliquefier would cost $560k. This includes a building to house compressors and a water cooling tower. It would include limited gas storage, equivalent to 760 gallons of liquid nitrogen, which is one forth the daily design production.

Table 6. Pay back Period.

Operating mode			Yearly costs in $1000 amounts			Pay back period in years
c	f	e	(3) c*f*80/e	(4) f*24	(5) f*240	(6) 1/(5-(2+3+4))
A 1.0	1.0	1.0	80	24	240	5.2
B 1.3	1.0	1.0	104	24	240	6.7
C 1.0	0.3	0.7	34	7.2	72	220
D 1.0	0.5	0.8	50	12	120	19

c is a power cost inflation factor, c=1 represents present power cost.
f is the fraction of design capacity actually needed in day to day operation.
e is an efficiency factor assumed to be 1 at design capacity and assigned somewhat arbitraryly for the values of f listed.

A: System is used at design capacity.
B: System is used at design capacity with power cost of 4.5c/kwhr.
C: System is used to satisfy present average need.
D: System used in transition period of cyclotron construction.

Table 6 shows the payback period achieved under a number of operating conditions. The yearly maintenance cost is arbitrarily assumed to be 5%

of the capital cost. Makeup liquid which would be bought commercially is assumed to be equal to 10% of consumption. The variables considered are f, the fraction of capacity actually used, e, an efficiency factor to account for lower efficiency of the plant when not operated at design capacity, and c, a factor to account for uncertainty in the cost of power.

To Summarize:

(1) Capital cost is $560k.

Yearly costs are as follows.

(2) Maintenance is assumed to be 5% of $560k=$28k.

(3) Power cost is c*f*$80k/e.

(4) Makeup liquid to be bought commercially is 10% of f*$240k.

(5) Cost of buying all liquid used in a year commercially is f*$240k.

(6) The pay back period is then given by Y=1/{5-(2+3+4)}.

One conclusion to be drawn from table 6 is that it may be more economical to purchase an undercapacity plant and to expect to satisfy peak loads by purchasing liquid commercially.

COST COMPARISON BETWEEN SUPERCONDUCTING AND CONVENTIONAL OPTIONS FOR BEAM LINE MAGNETS

A.F. Zeller and J.A. Nolen

In order to determine whether superconducting beam line dipoles and quads are competitive with conventional conductor magnets, we have carried out a comparison similar to that done for the S800 spectrograph.[1] The analysis has used the beam line quad and the 22.5 degree beam analysis dipole, described elsewhere in this report, as a basis for comparison with conventional magnets which are also calculated with POISSON. Comparison with the ±16 degree superconducting switching magnet is not made here, but its cost is expected to be similar to the 22.5 degree magnet.

Superconducting			conventional (3000 A/in^2)	
Construction:				
Iron	@ $1.5/lb 300 lbs	0.5 k$	3,900 lbs	6.0 k$
Conductor	@ $0.02/ft 50,000'	1.0 k$	385 kg @ $20/kg	8.0 k$
Power Supply	15 A, 10V	0.5 k$	46 kW	10.0 k$
Cryostat, Bobbin, Winding, Assembly		4.0 k$		
Cryogenic Plumbing		4.0 k$		
Refrigerator (fraction of larger system)	0.5 W	2.5 k$		
SUB TOTALS		12.5 k$		24.0 k$
Operational Costs (10 Years, Electricity @ $0.05/kwh)				
Electricity	(ref 0.5 kW)	2.0 k$	P.S. (10% duty factor)	20.0 k$
Maintenance		0.5 k$		
Cooling Water			9 gal/min	1.5 k$
Liquid nitrogen		1.0 k$		
SUB TOTALS		3.5 k$		21.5 k$
TOTALS		16.0 k$		45.6 k$
X 70		1120.k		3185.k$

Comparison of beam line quads is made in Table 1, where the costs are broken down into initial construction costs and operational costs over a 10 year period. The superconducting quad is described elsewhere in this report. The costs listed assume some savings for a production mode construction program. The refrigerator costs are based on a share of the whole Phase II refrigerator capacity and its operational cost assumes continuous use. The conversion ratio of 1 W cooling= 1 KW of electricity was used. These estimates are somewhat large, but this allows for cool-down cycles to be included in the refrigerator costs. We have assumed a current density of 3000 A/in^2 in the conventional coil with a 60% filling factor. Although a reduction to a more conservative 1000 A/in^2 reduces the power requirements by 50%, the large increase in iron and coil material costs greatly offsets this gain. Cooling water costs are only the amount of electricity needed to pump the water through the system, it assumes the cooling water system already exists. It should be noted that the conventional quad field quality is also not nearly as good as that of the superconducting quad.

Table II

Cost Comparison for 22.5 Degree Bend Dipole, 5 cm. gap, 1.2 m long, and 17.5 kG field. See Table 1 also.

Superconducting Window-Frame			Conventional Window-Frame		Conventional H-Frame	
Initial:						
Iron	2500 lbs	3.5 k$	19800 lbs	29.5 k$	1300 lbs	19.5 k$
Conductor	2200' (@ $.12/ft)	2.5 k$	289 kg	6.0 k$	232 kg	4.5 k$
Power Supply	750 W	1.0 k$	39 kW	9.0 k$	35 kW	8.0 k$
Cryostat, Winding, Bobbin & Assembly		6.0 k$				
Cryogenic Plumbing		4.0 k$				
Refrigeration 1 W		5.0 k$				
SUB TOTALS		22.0 k$		44.5 k$		32.0 k$
Operational costs (10 year)						
Electricity	ref. 1 kw	4.0 k$		17.0 k$ (10% duty factor)		15.0 k$ (10% duty factor)
Maintenance		1.0 k$				
Cooling Water			(8 gal. min.)	1.0 k$	(7 gal. min.)	1.0 k$
SUB TOTALS		5.0 k$		18.0 K$		16.0 K$
TOTALS		27.0 k$		62.5 k$		48.0 k$

Comparison of the dipole magnets is made in Table 2. Both conventional H-frame and window-frame are compared with the superconducting 22.5 degree window-frame. Similar assumptions to those used to calculate Table 1 are used here. The optimized superconducting H-frame is bigger than the window-frame, and more expensive. This is in contrast to the conventional cases listed in the table. A small gap, 3000 amp/in^2 (17.5 KG) window frame magnet requires much more area (i.e., a wider yoke than an H-frame which can gain room for the coil by expanding vertically and horizontally. Therefore, a conventional window-frame will be more massive than the corresponding H-frame. For a superconducting magnet at much higher curreent density, an H-frames will be more massive than a window-frame. As an example, the S-800 superconducting dipoles when designed as window-frame weighed ~ 50 tons each. They were subsequently redesigned as H-frame, with an approximate 40% increase in the mass.

It would seem that even for beam line quads and dipoles, the superconducting option is the cheapest. However, these designs are for devices which have large volumes of good fields or gradients ($\leq$ 0.1%). If less field quality is acceptable, then smaller versions of the conventional magnets can be built. There is little savings to be expected from scaling down the superconducting devices though, because costs are dominated by such things as winding, fabrication and plumbing, rather than material costs.

With these estimated costs for the magnets and refrigerator the total net savings with the superconducting beam line for Phase II is well over two million dollars for a 10 year operating period. The currently estimated costs of various options for distributing liquid He and liquid N_2 to the magnets is much less than this number.

---

1. J.A. Nolen, "Workshop on High-Resolution, Large-Acceptance Spectrometers", ANL, Sept. 1982, III-B.

CONDUCTION COOLED SUPERCONDUCTING MAGNET LEADS

A.F. Zeller, J.A. Nolen, Jr. and J. Bass*

In designing current leads for superconducting devices two opposing problems are encountered: 1) keeping the lead/cryostat as simple (cheap) as possible and 2) keeping the overall helium refrigeration load as low as possible. For open systems, which do not return gas to a refrigerator, vapor cooled leads which use the enthalpy of the helium gas are the obvious solution. For closed systems the choice is not so clear cut, when refrigerator operation efficiency is also included in the assessment.

Current leads which are not cooled by helium boil off obey the equation of state:

$$\dot{dQ}_i + I^2\rho(T)/S = 0 \qquad (1)$$

where

$$\dot{Q}_i = \lambda(T)S\, dT/dl \qquad (2)$$

with ρ and λ the temperature dependent resistivity and thermal conductivity, respectively. I, S, and dl are the current, cross sectional area and incremental length. The minimal heat flow into the cold end, $\dot{Q}_c$, is then

$$\dot{Q}_c = I\left[2\int_{T_{cold}}^{T_{hot}} \lambda(T)\rho(T)dT\right]^{1/2} \qquad (3)$$

This occurs when $\dot{Q}_H = 0$, i.e., only the resistive heat generated within the lead is carried into the cold bath.

Because of the strong dependence of both λ and ρ with temperature, the usual simplification assumes the Wiedemann-Franz-Lorenz (WFL) law:

$$\lambda(T)\rho(T) = LT \qquad (4)$$

where L is the Lorenz number with the Sommerfeld (L_o) value of $2.44 \times 10^{-8} V^2/K^2$. However, it is known that L is constant for pure metals only at very low and very high temperatures, with respect to the characteristic Debye temperature, θ_D, (see, for example ref 1 and 2). For the case considered here where the hot end is clamped at 77 K, the minimum Q is then

$$\dot{Q} = I\left[2\int_4^{77} L(T)T\,dT\right]^{1/2}. \qquad (5)$$

If L were constant and equal to L_o, then all pure metals would have a $\dot{Q}/l$ per lead of 12 mW/A, However, in the range $0.01 < T/\theta_D < 1$, the Lorenz numbers can have significant deviations below L_o. This is because the relaxation times for electron-phonon scattering for resistance and thermal conductivity differ, with the electrical resistivity decreasing faster with decreasing temperature than the thermal conductivity is increasing[1,2]. This deviation depends strongly on the electrical purity, i.e., the residual resistivity ratio (RRR). The larger RRR for a given material, the larger the deviation from L_o. This effect is shown in Fig. 1 for different purities of aluminum and for high purity copper and tungsten. The curve for copper was obtained from the compilation in ref. 2. Those for aluminum were constructed with data from ref 3 and 4 and for W from ref 3 and 5. They are plotted as a function of T/θ_D in figure 1 and as a function of T in figure 2. Additionally figure 2 shows a lower RRR copper curve.

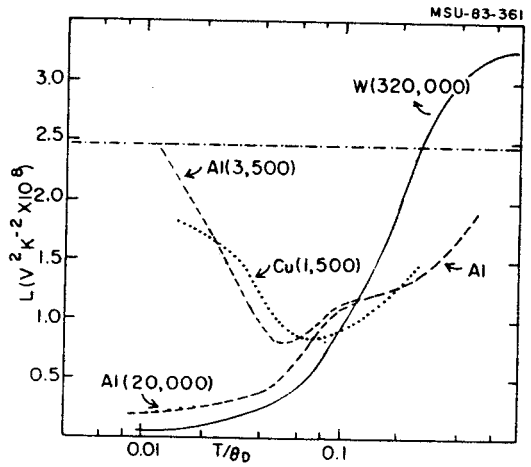

Fig. 1. Lorenz numbers as a function of reduced temperature, T/θ_D for Cu, Al, and W. The number in parenthesis is the RRR. The dashed-dotted line is the Sommerfeld value, L_o.

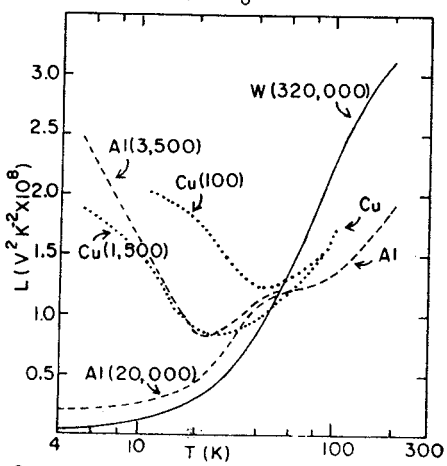

Fig. 2. As Fig. 1 but function of temperature.

The similarities between figures 1 and 2 point out the problem in finding a good material

for conductively cooled leads: while significant differences between materials, and between purities for a particular metal, may exist at lower temperatures, in the region of interest, 40-77 K, little difference is observed. Since the optimum $\dot{Q}$ depends linearly on T and as $L^{1/2}$, only temperatures close to the upper limit, 77 K, contribute to the integral. This shows up especially in the calculated results, a few of which are given in ref 6-8. Figure 2 also shows that the higher the purity of a given metal, the lower the $\dot{Q}$; a fact sometimes obscured because of the lack of ρ and λ curves for the same material. Table 1 in ref 7 illustrates this difficulty in properly matching ρ and λ since this compilation seems to show that a lower purity material has a smaller $\dot{Q}$ than that with a larger RRR. Table 1 lists $\dot{Q}$ calculated from curves shown in figures 1 and 2.

TABLE I

MATERIAL	$\dot{Q}$ (mW/A)	θ_D (K)*
W (320000)	8.4	405
Al (3500)	8.0	426
(20000)	8.0	
Cu (100)	9.1	344
(1500)	8.2	

*From Ref. 2

A closed refrigeration system can operate in two basic modes: 1) gas returning at 300 K is cooled and liquified or 2) gas returning at 4.5 K is reliquified. The refrigeration system at NSCL will have a capacity in mode 1 of 200 L/hr and in mode 2 of 800 W. For 100 magnets running at 100 A, the heat load for vapor cooled leads of the Efferson type[9] and gas returning at 300 K would use 14% of the 200 L/hr (2.8 mL/hr/amp per pair of leads). Purely conduction cooled leads of high purity aluminum with gas returning at 4.5 K would use 20% of the 800 W (16 mW/amp per pair of leads). Hence with these common materials the best nitrogen intercepted conductor cooled leads would cause about a factor of 1.4 more load on the refrigerator than the conventional vapor-cooled leads.

The reason that common metals give only marginally different results can be understood in terms of the Debye temperatures, given in table 1. Because the $\dot{Q}$ depends linearly on T, and only as $L^{1/2}$, the solution is seen to be one of shifting the minima of the curves in figure 2 to the right. This means, as implied in figure 1, finding a metal with a high θ_D and large RRR. Unfortunately, all the common metals have $200 < \theta_D < 450$.

One possibility exists, however, for a material which could give $\dot{Q}$ small enough to make conductively cooled leads competitive with vapor cooled leads: beryllium[2] has a θ_D of 1160 K. For a given RRR, the Lorenz numbers do not vary much between metals when viewed on a plot of T/θ_D, as in figure 1. It is possible to construct Lorenz numbers based on an assumed RRR[2]. Shown in figure 3 are curves for Be with differing RRR's calculated by this method. Also shown for comparison are Al and an experimentally measured curve for Be with RRR = 4 (99.5% pure). The shift

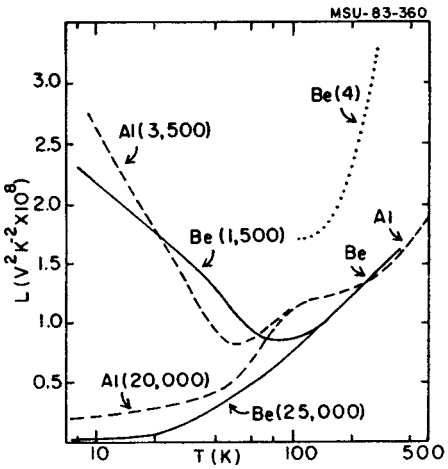

Fig. 3. As 2, but for Al and Be.

in the minimum L towards higher temperature results in a $\dot{Q}$ for the higher purity of 5 mW/A. Again using the case of 100 magnets, high purity Be leads would use only 12.5% of the 800 W capacity. Calculations for the less pure Be yield only 8mW/A. Because of the uncertainty in the method of estimating L, the actual values in high purity Be will probably lie between the two values. Nevertheless, the possibility of constructing simple leads competitive with vapor cooled leads is very encouraging. Of course, vapor cooled leads of Be could also be constructed, which would produce only 3/4 of the load of a conventional Cu lead.

Unfortunately, commercial Be wire of 99.8% purity was found to have RRR = 8. However, Be produced[10] in 1938 was observed to have RRR = 500, so producing Be of very high RRR is not out of the question, even considering its toxicity. We are presently exploring this possibility since the potential exists for producing lower heat leads, regardless of refrigeration mode. Such leads would also have application in the small self-contained cryogenic units discussed recently by Hoenig.[11]

* MSU Dept. of Physics

1. G.T. Meaden, "Electrical Resistivity of Metals", Plenum Press, N.Y. (1965).
2. J.G. Hust and L.L. Sparks, "Lorenz Ratios of Technically Important Metals and Alloys, NBS Tech, Note 634", NBS, Boulder, CO (1973).
3. Y.S. Touloukian, "Thermophysical Properties of Matter, Vol. 1, Thermal Conductivity, etallic Elements and Alloys", Plenum Press, N.Y. (1970).
4. J. Bass, "Electrical Resistivity of Pure Metals and Dilute Alloys" in "Landolt-Bornstein", New Series, Vol. 15a, "Metals: Electronic Transport Phenomena", K.-H. Hellwege, ed., Springer-Verlag, Berlin, (1982).
5. T.K. Chu, P.D. Desai, and C.Y. Ho, "Electrical Resistivity of Tungsten, CINDAS Report 74", Purdue University, W. Lafayette, IN, (1983).
6. M.C. Jones, V.M. Yeroshenko, A. Starostin, and L.A. Yaskin, Cryogenics 8:337 (1978).
7. Yu.L. Buyanov, A.B. Fradkov, and I. Yu. Shebalin, Cryogenics 15:193 (1975).
8. G. Aharmian, L.G. Hyman, and L. Roberts, Cryogenics 21:145 (1981).
9. K.R. Efferson, Rev. Sci. Instr. 38:1776 (1967).
10. E. Gruneisen and H.D. Erfling, Ann Physik 38 (5):714 (1938).
11. M.O. Hoenig, IEEE Trans. on Mag. Mag 19:880 (1983).

SUPERCONDUCTING TEST COILS

A.F. Zeller, J.A. Nolen, M. Dubois and J. DeKamp

Present designs for Phase II superconducting switching magnets, S800 beam analysis magnets and beamline quadrupoles involve potted coils. Therefore, we have undertaken tests of epoxy formulations and are constructing a cryotest stand to examine aspects of potted coils such as training, reproductibility of construction, and quench characteristics. Initial trials convinced us that a simple wet-winding (paint-as-you-go) technique, with random winding, was most efficient for constructing coils for the prototype dipole and prototype quad. Two epoxy formulas were tried, out of many cited in the literature, mainly on the basis of availability, curing temperature, strength, or on the experience of other labs. The two systems were:

1.) Epon 815/Versamid 140 plus 1-2% Silane 6020- a low viscosity, unfilled, clear epoxy which is cured for 24 hours at 75-150 degrees F, depending upon the portion of Silane added.

2.) Stycast 2850/Catalyst 11- a viscous, black, filled epoxy, which was heated to 70 degrees C to reduce the viscosity during application, and which sets in 2 hours @ 212 degrees F, followed by a four hour post cure[1] @ 300 degrees F.

Practice coils with ordinary copper wire of the appropriate size were wound with both the above forumulations. The cross sectional size is that to be used for the prototype dipole and consisted of 600-750 turns. After curing and removal from the winding fixture the coils were inspected for voids, then shock tested by repeated dipping in liquid nitrogen/warm water. Coils wound with the Epon 815 system were observed to have many large voids on the outside of the coil and cracked during shock treatment. The Stycast system survived repeated shock treatments with no cracks visible through 20X magnification and exhibited only small voids. Coils were then sectioned to check for packing and for internal voids. A cross section of one coil is shown in Fig. 1. Without epoxy 800 turns could be wound on the form, with the Epon 815 system 750 turns, and the Stycast 725 turns. On the basis of these trials the Stycast system was chosen for use.

Three coils using superconducting wire were wound. One coil with 600 turns of conductor destined for the prototype dipole, two with 800 turns of 0.5 mm diameter wire were wound. The two identical coils were found to have inductances identical to within a part in one thousand. One of the coils is shown in Fig. 2.

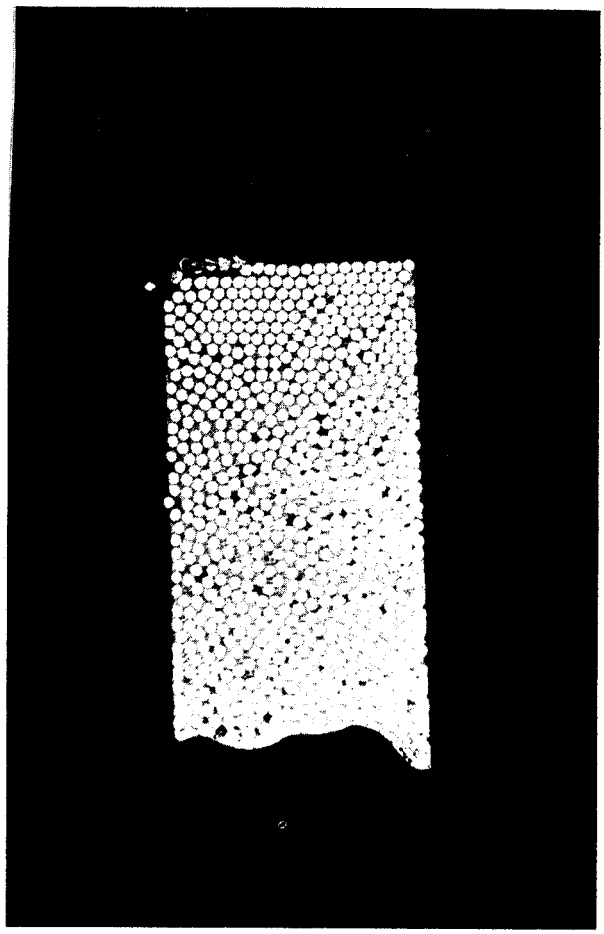

Fig. 1. Cross section of random wound test coil showing the close packing of the copper wire. The coil is approximately 1/2" by 1". Excess expoxy has not been removed nor have wires displaced during the sectioning been replaced.

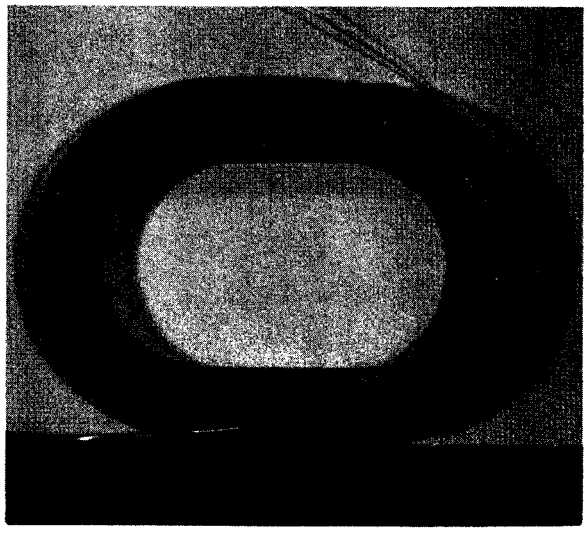

Fig. 2. Test coil before placement in support structure. The coil is approximately 6" in the long axis.

A mock up of the prototype dipole coil/helium containment system was constructed to test the coils in the cryotest stand. Fig. 3 shows a coil mounted in the fixture, before the top is bolted on.

Coil testing in the test stand is currently underway.

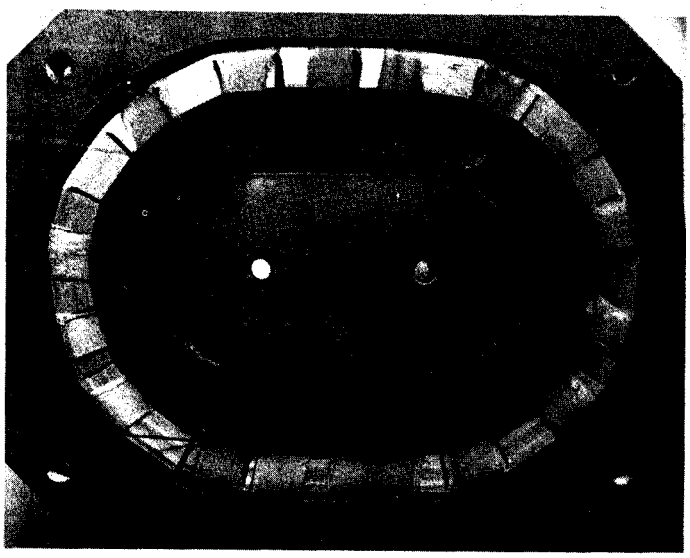

Fig. 3. Test coil in support structure. The helium channel is secured to the coil by spiral wrapping with scotchply.

1. W. Craddock, Fermi Lab, Private Comm.

SUPERCONDUCTING BEAMLINE QUADRUPOLE DESIGN STUDIES

A.F. Zeller and J.A. Nolen

Phase II operation will require approximately 70 superconducting quadrupoles for beam transport. Because of the large numbers involved, the necessarily high gradients needed for the Phase II rigidities, and the large apertures, we have tried to design an inexpensive quad which fulfills all these requirements and also generates minimum helium load on the cryogenic system.

Three types of quads were considered: 1) Panofsky[1] 2) intersecting circle approximations to a cos 2θ, and 3) hyperbolic poles.

The Panofsky quad, while easy to build[2], suffers from two problems: the field in the corners of a square quad is √2 times the field at the "pole". This means that the superconducting wire parameters are dominated by a region of "wasted field". The second problem is that Panofsky quads which have been built[3,4] have achieved the desired field uniformity only by very careful construction and attention to where each individual wire is placed. Thus, while Panofsky quads will probably be used for rectangular or very large aperture quads,[5] such as on the S800, the required care in construction precludes manufacturing them in a mass production mode.

Cos 2θ quads which produce highly uniform gradients of up to 50 T/m over a large volume have been built[6] at Fermi lab, and other places. However, this is convenient only if the conductor is a flat cable (approximating a current sheet) which requires high current operation (1000-5000 A). Current leads for 1000 A use 2.8 L/hr, so 70 quads would use all the 200 L/hr capacity of the refrigerator. Additionally, the cost of 70 high current power supplies is prohibitive. We have calculated quads which would use small diameter conductor wound to form two offset circles of current ("sliver quads") to approximate the required current density and shape. While quads of highly uniform field can be designed, they depend critically on exact wire placement. Small errors in coil placement result in large errors in the field.

Since it is easier to shape iron than complicated coil bundles, we have arrived at a design which shapes the field primarily by iron pole tips. We know that a window-frame dipole, in the infinite permeability limit, produces a perfect field up to the coil, the same dipole conformally mapped into a quad should also be perfect. The mathematical result is a hyperbolic pole and a coil which has hyperbolic faces and a nonuniform current density. Conventional copper coil quads which approximate this geometry have been used for a long time, but the problem of getting enough conductor into the space available has limited their use to low gradients or small apertures (see contribution on cost comparison in this report). Superconducting coils, of course, are not limited by the available space since the current density can be 50 times larger than in ordinary copper coils. Starting with a hyperbolic-shaped pole and coil, an approximation was found which relaxed the strict hyperbolic requirement for the coil and allowed some simplification of the pole shape. The calculated shape and field lines are shown in figure 1 for a 5" inside diameter quad. These calculations were

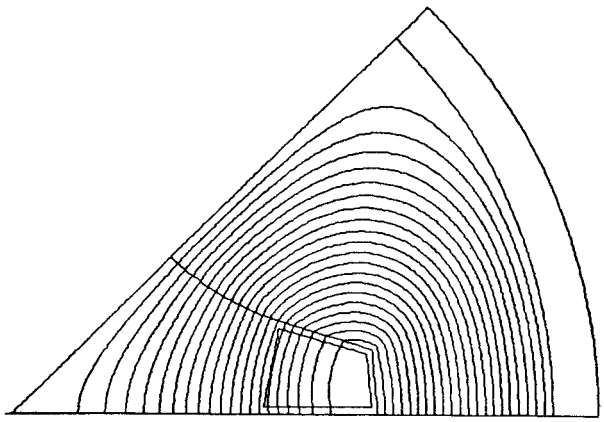

Fig. 1. Hyperbolic pole tip quad showing field lines and coil shape.

done with the two dimensional code POISSON and, therefore, do not include estimates of the end effects on the integral gradients. The hyperbolic edges of the coil have been approximated by straight lines at the indicated angles. The final radial position of the coil is a compromise between small radii to minimize the peak fields and larger radii to reduce sensitivity to details of coil placement. Figure 2 shows the uniformity of the gradient for the infinite permeability case and for several gradient levels in the finite permeability case. Beyond 7.3 kG/in (28.5 T/m) the field quality rapidly deteriorates as the poles saturate. Only at the highest gradients does the gradient error exceed 0.1% at a 2" radius. Table 1 lists the components of the field calculated at a 2" radius relative to the quad field in parts in 10^4, where the design has been optimized for 6 kG/in. Small changes in coil placement and/or shape did not produce large changes in the gradient properties.

In order to keep the helium load as low as possible, a small wire and low operating current wire chosen. The magnet, conductor, and coil characteristics are summarized in Table 2. Construction of the prototype guadrupole should begin this fall.

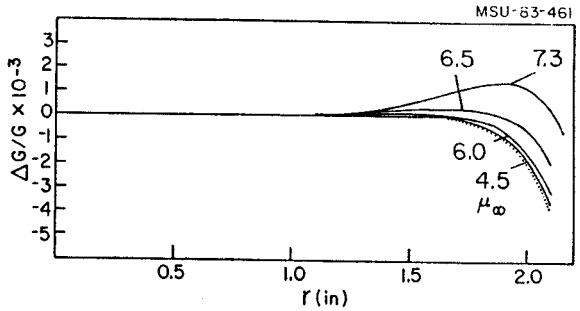

Fig. 2. Deviation of the gradient from the central gradient in parts per thousand as a function of radius. Calculations were done for various gradients (in kG / in) as indicated.

1. L.N. Hand and W.H. Panofsky, Rev. Sci. Instr. 33, 927 (1959).
2. J.R. Purcell, S.T. Wang, R.C. Niemann, K.F. Mataya, H. Ludwig, and J.A. Biggs, IEEE Trans. on Mag. Mag-11,455(1975)
3. R. Auzolle, F. Kircher, and J.P. Penicaud, IEEE Trans. on Nucl. Sci. NS-28, 3228 (1981).
4. K. Tsuchiza et al, NIM 206, 57 (1983).
5. L. Harwood, "Workshop on High-Resolution, Large-Acceptance Spectrometers, ANL", 1981, III-D.
6. W.E. Cooper et al., IEEE Trans. on Mag. Mag-19, 1372 (1983) and ref. therein.

TABLE 1

Harmonic analysis for components of the field at a radius of 2" for several gradients. The numbers are defined by $B_N/B_{quad} \times 10^4$. N is the component whose radial dependency, r, is given by $(1/r)^{(N-1)}$. λj is the current density in the coil at given gradient.

G (kG/in)	λj (A/cm^2)	N=6	10	14	18	22 ($\times 10^{-4}$)	Sum
μ=∞		1.0	-0.8	-0.7	-0.3	-0.1	-0.9
4.5	5400	1.2	-0.8	-0.7	-0.3	-0.1	-0.7
6.0	7300	1.4	-0.5	-0.7	-0.3	-0.1	-0.2
6.5	8000	2.5	-0.1	-0.7	-0.3	-0.1	1.3
7.3	9100	4.6	0.9	-0.7	-0.3	-0.1	4.5

TABLE 2

MAGNET			
Diameter (cold)	5"	Coil at 7.3 kG/in level	
Free bore (warm)	4"	I_{op}	12.5 A
Length of Iron	14"	Stored energy	6250 j
Outside diameter of yoke	12"	Inductance	77 h
Iron weight (cold)	320 lbs.	Helium gas for leads	0.035 L/hr
WIRE (NbTi)			
Diameter	0.3 mm		
Cu:SC	6:1		
I_{crit} @ 2T	18 A		
Turns per coil	3740		

SUPPORT LINKS FOR THE ±16° BEAMLINE MAGNET

M.J. Dubois, A.F. Zeller and J.A. Nolen

The coil and bobbin of the ±16° beamline magnet must be rigidly supported within the magnet's cryostat. The supporting elements must be strong enough to withstand 1800 lbs., which is approximately the worst case of unbalanced loading that will occur if one coil quenches. At the same time, the supporting structure must transfer a minimum amount of heat to the bobbin, which is cooled by liquid helium.

Due to the nature of the bobbin and cryostat of the ±16° switching magnet, the bobbin must be supported at its four corners. (Fig. 1) At each corner the bobbin is supported vertically by two links and horizontally by a single link, which is angled 45° from the center line of the bobbin. This configuration will provide adequate vertical support, and prevent twisting of the bobbin in the horizontal plane.

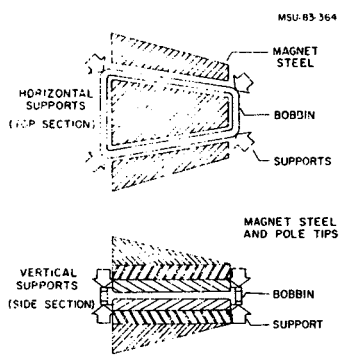

Fig. 1. Support link positions for the ±16° dipole in the horizontal and vertical planes.

Support Link Configuration

Various materials and configurations of both tension and compression members were studied. The result of these studies is the compression link shown in Figure 2. The link consists of a 0.25 inch diameter Glastic rod[1] which is in compression between the bobbin and a stainless steel jacket. This jacket acts as a connection to the liquid nitrogen shield and as a tension member to support the two compression elements. The outer link element is a cylinder of G-10 or similar epoxy-glass composite with a 0.75" outside diameter and a 0.0631" wall thickness.

The ends of the link are capped with stainless steel end restraints to prevent splitting of the glass fibers and to act as a rest surface for the support pins. The support pins have spherical surfaces to allow the link to skew to small angles (up to 5°). This prevents shear and uneven loading. To facilitate assembly, the link components are glued together with commercial superglue (Elmers wonderbond cyanoacrlic adhesive).

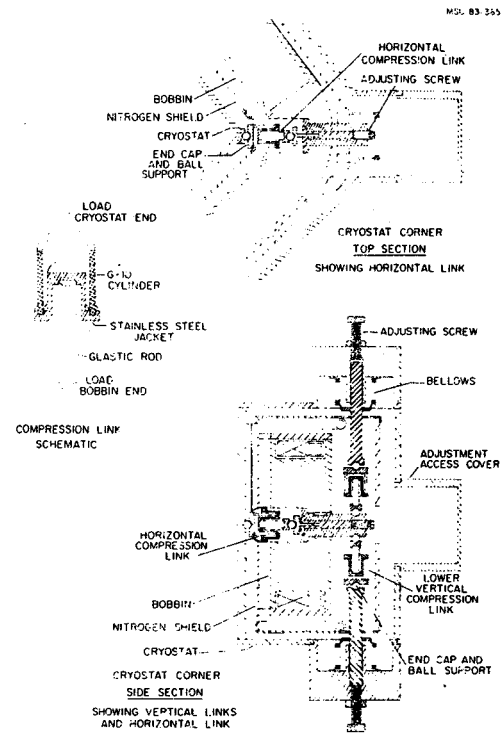

Fig. 2. Details of support links.

Loading

The compressive strength of the Glastic rod was verified by "in house" testing to be approximately 100,000 PSI at room temperature (300° K). When cooled to 77° K, the strength of Glastic improved by a factor of 2. As used in compression, Glastic proved sensitive to surface irregularities, requiring a flat, smooth mating surface between the two materials under compression. To achieve this mating surface, and to prevent splitting of the Glastic, the ends of both the Glastic and G-10 were restrained perpendicular to the load by fitting the cylinders in a reamed hole. To closely fit the cylinders into such a reamed hole, the mating surfaces of the intercept and the restraining end caps were machined carefully to close tolerances. In prototype models of the link, this was achieved with standard machining practices, and posed no special problems.

For the 0.250" dia, Glastic rod, the working strength is 4900 lbs at 300° K, or approximately 9800 lb at 77° K. The worst case load on the link

will be 1800 lbs. This gives a safety factor of 5.4. This factor may be reduced considerably in future tests in order to lower the total liquid helium usage, as discussed below.

The G-10 cylinder has properties which are well known, and were not tested extensively before prototype construction. Other composite materials are being considered which would offer higher strength and lower thermal conductivity. The G-10 cylinder was tested to a load of 3000 lbs.

Link Configuration, Spring Loading and Deflections

If compression links are placed on the inside of the bobbin, thermal contractions at operational temperature (4° K) will cause the bobbin to be rigidly supported horizontally. The contractions are approximately 0.065 inches at each corner. This amount of contraction on the link alone would require a load that would cause failure. Loading the horizontal link with Belleville spring washers will allow the link to support the bobbin firmly at room temperatures. As the bobbin cools, the washers flatten until they "bottom", thus absorbing the majority of the thermal contractions. At operating temperature the link is firmly seated against the bobbin. Stock Belleville washers are available that satisfy these requirements.

The vertical links support the bobbin at its midplane, and are affected only by thermal contractions of the link itself. These can be compensated for by pre-loading the link at room temperature before cooldown. Based on samples tested, each link will contract approximately .0013 inches.

Deflection of 0.0013 inches can be obtained with a pre-load of 400 lbs. Then, as the link cools and contracts, this pre-load will maintain contact as the link loading decreases to about 100 lbs.

For the prototype switching magnet, the loads on the links can be read using flat force transducers. If the absolute load is not required, but only alignment information is needed, simple strain gauges placed strategically on the cryostat could provide this information.

Heat Transfer

The heat transfer calculated for the links is based on data from the manufacturers of Glastic and G-10. For materials with a temperature dependent thermal conductivity, the heat transfer between two surfaces is the finite integral of thermal conductivity between the boundary temperatures times the ratio of the area to length of the conduction path, or

$$Q = \frac{A}{L} \int_{T_1}^{T_2} \lambda dT$$

The integral of thermal conductivity for G-10 was used to evaluate both sections of the link. For the Glastic rod, the integral of thermal conductivity is 0.172 W/cm between 4° K and 77° K. For L = 0.75 inches (1.91 cm) and a diameter of 0.25 inches (A = 0.317 cm^2) the heat transferred to the liquid helium system is 0.029 Watts/link. For the 12 links of each switching magnet, the support links impose a heat load to the liquid helium system of 0.34 Watts/magnet. At present time, the possibilities of reducing this heat load further are being studied. This might be achieved by reducing the cross sectional area of the link or increasing the length. The strength requirements given tend to be conservative, and possibilities of reducing the overall strength of the link are also being considered. A proposed goal is a helium heat load of 0.2 W for the entire magnet in order to approximately match the boil off rate required to run the vapor-cooled current leads.

Similarly, the thermal conductivity integral is 1.3 Watts/cm for G-10 between 77° K and 300° K. For a 0.75 inch diameter, 0.0625" wall cylinder (A = .871 cm^2, L = 1.91 cm) the load imposed on the liquid nitrogen system by the support links is 0.58 Watts/link or 7 watts total. This load results in a boil off of 0.15 liters/hour of liquid nitrogen.

Summary

A compression link made from epoxy-glass composite materials is feasible and has been built and tested. The link has excellent strength, verified to withstand a load of 3000 lbs. at room temperature. The link has a low rate of heat transfer, calculated to be 0.029 Watts/link to LHe. Methods of reducing this value are under study. The load on the LN_2 system is calculated to be 0.58 Watts/link.

The links pose no unusual machining or manufacturing problems, and are relatively inexpensive, compact and lightweight. The use of compression links also simplifies construction of the dipole cryostat, since the cryostat may be built from the "inside-outwards". The apparent feasibility of this link configuration has led to consideration for further application in other beamline components such as quadrupole and steering magnets.

1. The Glastic Company, Cleveland, Ohio 44121

DESIGN STUDIES FOR THE 22.5 DEGREE BEAM ANALYSIS SYSTEM MAGNET

A.F. Zeller and J.A. Nolen

A preliminary design for the 22.5 degree beam analysis system dipole magnets, four of which will be needed to get the beam into the S800 pit, has been completed. Since the magnets differ from the ±16 degree switching magnets in that they only operate at a fixed bend angle (the beam never goes through them when they are turned off), the economical solution of rectangular magnets is to have the beam enter and exit at an 11.25 degree angle. This uses the largest fraction of good field available without the complication of winding a coil having a negative curvature which follows the beam sagitta.

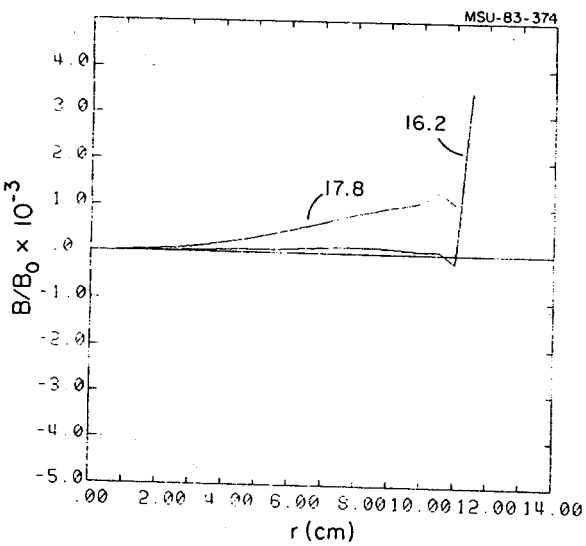

Fig. 1. Field uniformity for cold mass window frame 22.5 degree magnet as calculated by the program POISSON. The coil edge is 15 cm from the center.

The design calls for a window frame geometry with a 5 cm gap. The design goal is a field uniformity, $\Delta B/B_o$, of 0.1% out to a distance of 11 cm on either side of the midline at a field strength of 17.5 kG. Figure 1 shows the calculated results for a field below and slightly above 17.5 kG. Above 17.8 kG, the field quality rapidly deteriorates. Bending a K = 1200 beam requires a length of 1.2 m, resulting in a cold mass (the entire magnet) of 2500 lbs. The maximum current density at 17.5 kG is 13,500 A/cm^2.

Because of the difficulties in winding a saddle coil and having a large cold mass, with its associated long cool down time, we have investigated cold and warm H-frame geometry magnets. However, none of the designs met the field uniformity requirements without significant increases in the iron mass. One of the big advantages in the cold mass design is that it readily lends itself to incorporation in a modular bend unit, [1] which also simplifies the cryogenic distribution system. Feasibility studies are presently underway to determine if the alternate designs are cost competitive with the simple window frame design when both material and labor costs in construction and in the associated cryogenic system are considered.

1. J.A. Nolen, "Workshop on High-Resolution, Large-Acceptance Spectrometers, ANL", Sept. 1981, IV-F.

STUDY OF THE SENSITIVITIES OF THE MAGNETIC CENTER OF A MAGNET TO INACCURACIES IN THE FABRICATION OF THE MAGNET YOKE

L.H. Harwood, J.A. Nolen, and H.G. Blosser

For the construction specifications of a magnet to be made, one must know the tolerances of the various surfaces. To get these tolerances one needs to know the sensitivities of the field to changes in the various surfaces. Likewise, when magnet iron is delivered with inaccuracies in production, one needs to know these sensitivities before investigating correction of the errors. The present study was done to investigate some of these sensitivities.

The model used in the calculations was an infinitely long "H" frame dipole. Such a magnet is calculable with POISSON. First, a perfectly symmetric magnet was calculated. Then, changes were made in the positions of various surfaces of the magnet and the field was calculated for the new configuration. Three parameters were extracted from each calculation: 1) the position of the magnetic center of the magnet was obtained by fitting the field near the geometric center fo the magnet with a parabola, 2) the "first harmonic" of the magnet, (B(right)-B(left))/2, was calculated at the point where the field starts to have a large gradient (2.67 in. from the center), and 3) the "first harmonic" was calculated at the edge of the pole tip (4.0 in. from the center). The field was not varied in the calculations; the central field was 1.9 T and the field in the iron was 2.1 T.

The results of the calculations are summarized in Table I. For each configuration, the result for the symmetric magnet was subtracted from the result in order to remove artifacts of the calculation as much as possible. Eight cases were examined; the first set of cases examined basic sensitivities: 1)all of the iron was displaced (the coil remained stationary, 2)the outer surface of the left yoke was moved outward, 3)the inner surface of the left yoke was moved inward, and 4)the entire left yoke was moved inward. The initial result was that the position of the inner surface of the iron was most critical in determining the magnetic center of the magnet; while this is quite expected at low fields, it was somewhat surprising with saturated iron. The next two cases tested the sensitivity of our result to the positions of the coils: 5) the yokes of the magnet were moved in close to the coil and the inner surface of the left yoke was moved an additional distance in and 6) with the yokes in their original configuration, the coils were moved out to near them and the inner surface of the left yoke was moved inward. As a check, mirror symmetric versions of cases 5 and 6 were run with the result that our procedure gave an essentially correct reflection of the physics with little or no calculational artifacts, the 40 G difference between the 1st harmonics in cases 5 and 7 is only significant discrepancy and occurs at a point where the field gradient is about 5 kG/in. These cases indicated that the magnitude of the asymmetry was most affected by the distance from the center to the yoke and not to the level of saturation in the iron near the yoke.

The essential conclusion of this study is that in specifying and inspecting magnet iron that it is the inner surface that is most important. Errors in the position of the outer surface only affect the net saturation of the magnet and thus only the field-vs-current relation.

Magnet Asymmetry Study Results

Case #	What Moved	How far (in) (1)	Center motion (in) (1)	1st harm. 2.67 in from center (G)	1st harm. 4.0 in from center (G)
I	All iron	-0.25	-0.045	-14.5	-45
II	Outer surface of left yoke	-0.025	0.0	0.0	-2.5
III	Inner surface	+0.25	+0.030	+9.5	+28.
IV	Entire left yoke	+0.25	+0.027	8.5	26.
V	Widen both yokes inward; move inner surface of left yoke extra	+0.25	+0.100	43.	131.
VI	Yokes in orig. positions move coils out near yokes. Move inner surface of left yoke	+0.25	0.027	8.5	26.
VII	Mirror of V		-.100	-40.5	-173.
VIII	Mirror of VI		-.050	-6.5	-33.

1) The sign convention is such that a negative motion is to the left.

R.F. - CORRELATED X-RAY PRODUCTION: A POSSIBLE TECHNIQUE FOR DEE PHASE TIMING

R.M. Ronningen, M.L. Mallory, and R.A. Blue

Electrons move in the high voltage gradients between the dees and between the dees and ground in the K500 cyclotron. Thus, bremstrahlung radiation is produced, and indeed the end-point of the spectrum is used to calibrate the dee voltages.[1] We observed the time spectrum of x-rays in coincidence with RF pulses.

X-rays produced by dee excitation voltages of 30-60 keV were observed by a 2 in. x 2 in. plastic scintillator coupled to an RCA 8575 phototube. Anode signals were processed using constant fraction timing and these pulses started on time-to-amplitude converter (TAC), stopped by RF pulses. The TAC spectra, an example of which is shown in Fig. 1, showed peaks indicating that the X-ray production is time-correlated with the R.F.

In first harmonic operation the phase difference between the voltages applied to each pair of dees is 120 RF degrees. A precisely centered accelerated beam requires the dee phase to differ by less than 1° RF (which is near the limits of electrical phasing) from the 120° phase difference. One should be able to achieve this accuracy using the above fast nuclear timing technique (≤1 nsec). The centroids of the time distributions can be routinely determined to an accuracy of better than 1° RF. Centroid shifts depend upon relative dee voltages and phases. Efforts are now underway to understand those relationships.

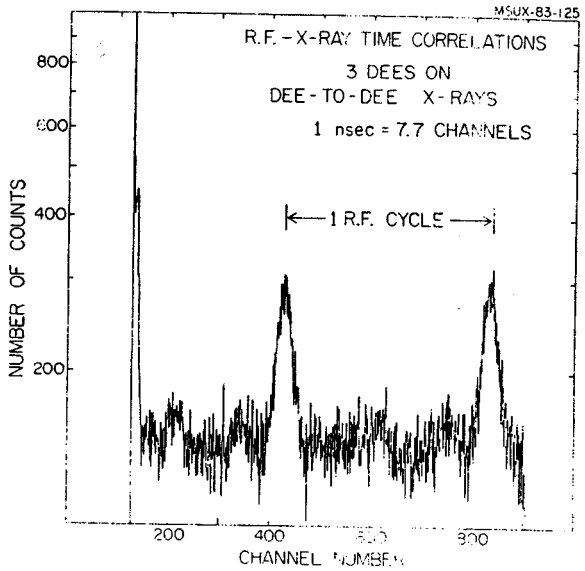

Fig. 1. Time-to- amplitude converter spectrum of x-ray-RF correlations. A spectrum doubler was used so that 2 RF cycles could be observed. X-rays are thought to be produced by electrons accelerated in the inter-dee high voltage gradients (dee-to-dee x-rays) rather than gradients between dees and ground (ion source).

1. Peter Miller and Edwin Kashy, Proc. 7th Int. Conf. on Cyclotrons and their applications (Birkhauser, Basel, 1975) p. 171-174.

TRANSGRAPH: AN INTERACTIVE ION-OPTICS CODE USING COLOR GRAPHICS

L. HARWOOD

The design of the K500-K800 coupling line proved to be a unique set of fitting criteria from many of our other design projects. We needed to fit the coupling line into an area that was rather confined and simultaneously achieve the optical feat of matching the K500 emittance into the K800 acceptance while keeping the pulse length constant. The optics program to be used, TRANSPORT, provided only numerical output. Thus, if the bend angle of a dipole or the length of a magnet or drift space were changed, the effect on the physical layout of the system would only be discernable after tediously plotting the output coordinates by hand. An interactive program with graphic output would much simplify the design procedure. An AED-512 color graphics unit had recently been acquired by the laboratory; this seemed the ideal unit for the purpose. Thus, the program TRANSGRAPH (TG) was written. The following is a brief description of this program.

TRANSGRAPH (TG) is an interactive ion-optics code which uses an AED-512 color-graphics unit for user interaction. The basis for TG is TRANSPORT (TP) and as such will do most functions that TP is capable of; not all options are available (mostly printed output options). The main goal of TG is to permit the user to have rapid turnaround and easily interpretable output from TP. Graphic output includes a plan view of the system and plots of 1st order matrix elements and beam envelop sizes. Interactive input consists of adding, deleting and modifying elements in the system. The optics calculation takes the same length of time that TP would have taken without the graphics; the graphics display takes 1-5 seconds depending on its conplexity and on which VAX the program is running. Currently the communication to the AED is on a parallel link, but switching to a serial, terminal link would not involve software modification or cost a great deal of interaction time when in use.

The TG display has three major regions. The upper half of the screen gives a plan view of the "world". The non-TP-calculated world is drawn with grey lines. The TR world is done in color: drifts are white lines, quads are green, dipoles are red (solenoids, sextupoles, etc. are also included with their own colors). Zero length elements (edge angles, fitting constraints, etc.) are not (and cannot be) illustrated. The lower half of the screen has the plots of the matrix elements and beam envelop (TR "sigma" matrix) sizes. To simplify correlating the plots with the elements in the system, the system is displayed in a linear form on the border between the two plotting areas. Five matrix elements are plotted in different colors (on a black background) above the system. The identity of each is given on the right. The scales for the different plots can be different, so the scale for each element is given also. Below the system, the envelops are plotted in blue on a grey background.

There are three smaller regions of the screen which are also used but for alphanumeric I/O instead of graphic information. The upper right of the screen, outside the display, is used to output all non-zero values of the transfer matrix upon request. Below this region, as described above, is an area used to provide information pertinent to the plots. The region for all alphanumeric input is at the bottom of the screen. How input works is described below.

TG uses a set of input files; these include the initial-guess TP input file, a list of matrix elements to be plotted, and the geometry of the "world" in which the problem exists (shielding walls, pits, etc.). TG also generates a set of output files: a TP output file (suitable for printing) and a listing of the current system (suitable for use as a TG or TP input file after minor changes).

TP is a very powerful program with many options. Many are not enhanced and/or are not compatible with graphic output (misalignment results, for example). Also, the real goal of the program is zero and first-order designs; therefore TG does not do second-order calculations. Likewise, the graphic thrust of the program minimizes the need for printed output, therefore the printing options are not extensive. Aside from these restrictions, TG closely reproduces TP. For those options not available in TG, the user can resort to TR. The capability to generate a file with TG which needs little modification to become a proper TR input file is addresses these limitations in a rudimentary fashion.

After generating the necessary files and making the appropriate assignments, you are ready to run TG. TG will execute the TR input file exactly as if it were TR (including coupled parameters during fitting) and then generate a complete display. All options of TG are then available. Elements may be added or deleted at any point in the system. Any parameter of any element can be changed. The choices of matrix elements may be changed. Fits may be done. The complete transfer matrix at any point can be shown. Different fitting conditions for a given system can be saved and recalled. Intermediate solutions can be saved and recalled.

To achieve the above, one must be able to give TG instructions. This is straightforward. The selection of an option is made by typing in the mnemonic for that option. If the desired function requires a position definition in the

"world", e.g. selecton of an element is the system then the cursor is placed at this location before typing in the name of the function. The function will then be executed. If the function does not need a position, then the location of the cursor is irrelevant. Functions which need additional input prompt for it.

To date, the systems designed with this program are the K500-K800 coupling line and the K500 beam lines. Studies have also been done for an RPMS at the LBL Bevalac.

Program development is ongoing. As it is used, more options become desired and one has a better idea of the way an option should work. These improvements are incorporated whenever possible. A writeup for this program is presently in the works, and should be finished before the end of the summer.

CYCLOTRON ORBIT THEORY

M.M. Gordon

The first stage of the work described in last year's Annual Report on the canonical treatment of accelerated orbits in cyclotrons was completed and written up in a paper which will appear in Particle Accelerators. This paper includes a further development of the theory which occurred after last year's report, namely, a generalization of the analysis to cyclotrons with spiral electric gaps.

As a separate project, we have undertaken the preparation of reports presenting a fairly complete discussion of the theoretical basis for some of our orbit computation programs. The first of these, entitled "Calculation of Isochronous Fields for Sector-Focused Cyclotrons", was completed last summer and has recently appeared in Particle Accelerators.[1]

A second report dealing with the calculation of closed orbits and basic focusing properties is nearing completion. This work describes in detail a proposed new version of the program "Cyclops" which is a sophisticated form of the Equilibrium Orbit Code. In addition to calculating the focusing frequencies ν_r and ν_z, Cyclops can provide more detailed information on the linear oscillations including, for example, the form factors and eigenellipse properties.

Assuming adiabatic acceleration, this information allows one to calculate, in particular, the vertical extent of the beam as a function of both r and θ for a given acceptance, and since the vertical extent is actually limited, these results serve to fix the vertical acceptance for each operational configuration of the cyclotron. Such calculations provide a more realistic estimate of the focusing limits than does the simple condition $\nu_z = 0$.

The new Cyclops program is also designed to generate linear transfer matrix elements for median plane motion including the time coordinate, and also for vertical motion. These data can then be used in another (as yet unwritten) program which very rapidly calculates large groups of accelerated orbits assuming the motion is linear but not necessarily adiabatic. Such a transfer matrix program, named "COMA", has been developed and successfully used at the TRIUMF laboratory, and before writing our own program, we will first try to adapt COMA for use with spiral electric gaps.

Another project completed last year concerns an analysis of the effects of asymmetric dee voltages or phases on the radial oscillations, particularly at the $\nu_r = 1$ resonance. These effects are important for superconducting cyclotrons (and many other cyclotrons) since they frequently operate with ν_r close to unity, and must actually accelerate the beam through the $\nu_r = 1$ resonance in the central region and again just prior to extraction. The dees in these machines are designed to operate in a symmetric configuration with equal voltages and prescribed phases because deviations from these values produce an asymmetry which perturbs the radial oscillations.

We should first note that cyclotrons with two or more dees are very common, and the operators of these machines soon learn that the "centering" of the beam can be manipulated by changing the voltage of one dee or shifting its phase relative to the other dee or dees. Although this effect is generally understood to be associated with the $\nu_r = 1$ resonance, an analysis of this phenomenon has not previously been carried out. We should also recall that many cyclotrons are equipped with a set of first harmonic magnetic bump coils which are routinely used to adjust the centering of the beam as it passes through the $\nu_r = 1$ resonance. Evidently, an asymmetry in the dee voltages or phases provides an alternative mechanism. The results of our analysis are therefore formulated so as to compare the effectiveness of the electric and magnetic perturbations.

There are two different gap crossing effects which can perturb the radial oscillations, and our analysis includes both. The first effect is produced by the outward shift of the equilibrium orbit as a result of the energy gain, and this effect occurs in all cyclotrons. The second effect is associated only with machines like the superconducting cyclotron which have spiral electric gaps and which therefore impart a radial impulse to the ions at each gap crossing.

Consider, for example, our K500 cyclotron where the beam traverses $\nu_r = 1$ at about r = 4 inch in the central region, and again at about r = 25 inch just prior to extraction. Since the spiral of the gaps is linear, the effect of this spiral is about six times greater at the outer radius. Despite this factor, the gap crossing perturbations turn out to be far less significant in the extraction region because they also vary inversely with turn number, and hence as $1/r^2$. Moreover, this factor makes the gap crossing perturbation very effective in the central region where the spiral is pratically negligible.

Our superconducting cyclotrons have three dees with an angular width of 60°, and in this case, we find that the form of the perturbation is extremely flexible. Indeed, it provides as much flexibility (at least in the central region) as can be obtained from the magnetic field bumps in use here and elsewhere. That is, the three dee voltages can be adjusted so that, without altering the net energy gain, they will produce an orbit

center displacement whose magnitude and direction can be varied independently.

A fairly detailed discussion of this analysis appears in a paper presented at the 1983 Particle Accelerator Conference held in Santa Fe.[2] The results are quite general and can be applied to any cyclotron although the specific examples given in the paper concern our own cyclotron specifically.

1. M.M. Gordon, Particle Accelerators 13, 67 (1983).
2. M.M. Gordon, IEEE Trans. Nucl. Sci. NS-30, 2439 (1983).